

AD_____

Award Number: DAMD17-99-1-9073

TITLE: Research Training Program in Breast Cancer

PRINCIPAL INVESTIGATOR: Daniel Medina, Ph.D.

CONTRACTING ORGANIZATION: Baylor College of Medicine
Houston, Texas 77030

REPORT DATE: July 2001

TYPE OF REPORT: Annual Summary

PREPARED FOR: U.S. Army Medical Research and Materiel Command
Fort Detrick, Maryland 21702-5012

DISTRIBUTION STATEMENT: Approved for Public Release;
Distribution Unlimited

The views, opinions and/or findings contained in this report are those of the author(s) and should not be construed as an official Department of the Army position, policy or decision unless so designated by other documentation.

REPORT DOCUMENTATION PAGE

Form Approved
OMB No. 074-0188

Public reporting burden for this collection of information is estimated to average 1 hour per response, including the time for reviewing instructions, searching existing data sources, gathering and maintaining the data needed, and completing and reviewing this collection of information. Send comments regarding this burden estimate or any other aspect of this collection of information, including suggestions for reducing this burden to Washington Headquarters Services, Directorate for Information Operations and Reports, 1215 Jefferson Davis Highway, Suite 1204, Arlington, VA 22202-4302, and to the Office of Management and Budget, Paperwork Reduction Project (0704-0188), Washington, DC 20503

1. AGENCY USE ONLY (Leave blank)	2. REPORT DATE July 2001	3. REPORT TYPE AND DATES COVERED Annual Summary (1 Jul 00 - 30 Jun 01)
----------------------------------	-----------------------------	---

4. TITLE AND SUBTITLE Research Training Program in Breast Cancer	5. FUNDING NUMBERS DAMD17-99-1-9073
---	--

6. AUTHOR(S) Daniel Medina, Ph.D.

7. PERFORMING ORGANIZATION NAME(S) AND ADDRESS(ES) Baylor College of Medicine Houston, Texas 77030 email dmedina@bcm.tmc.edu	8. PERFORMING ORGANIZATION REPORT NUMBER
---	--

9. SPONSORING / MONITORING AGENCY NAME(S) AND ADDRESS(ES) U.S. Army Medical Research and Materiel Command Fort Detrick, Maryland 21702-5012	10. SPONSORING / MONITORING AGENCY REPORT NUMBER
---	--

11. SUPPLEMENTARY NOTES Report contains color	20011127 011
--	--------------

12a. DISTRIBUTION / AVAILABILITY STATEMENT Approved for Public Release; Distribution Unlimited	12b. DISTRIBUTION CODE
---	------------------------

13. Abstract (Maximum 200 Words) (abstract should contain no proprietary or confidential information)
The goal of this research training program is to produce highly qualified scientists for careers as independent investigators in the field of breast cancer. During the last 25 years, there has been a fundamental revolution in the understanding of molecular and cell biological concepts related to cell growth, function and tumorigenesis. To utilize what has been learned and to continue future progress in the area of breast cancer requires the continued availability of well-trained, innovative and committed scientists. This program represents an interdepartmental training program involving 15 investigators from seven departments. Trainees are predoctoral and postdoctoral fellows with backgrounds in biochemistry, cell and molecular biology, molecular genetics and molecular virology. The training program provided trainees with additional foundation in carcinogenesis and breast cancer. In addition to the core curriculum taken by the predoctoral fellow in their respective academic departments, program enhancement is provided through trainees' participation in a graduate course on "Molecular Carcinogenesis" (predoctoral fellows), a Breast Disease Research Seminar (all trainees) and participation at national meetings and local seminars. Three predoctoral and three postdoctoral trainees are enrolled in the program.

14. SUBJECT TERMS breast cancer	15. NUMBER OF PAGES 42
	16. PRICE CODE

17. SECURITY CLASSIFICATION OF REPORT Unclassified	18. SECURITY CLASSIFICATION OF THIS PAGE Unclassified	19. SECURITY CLASSIFICATION OF ABSTRACT Unclassified	20. LIMITATION OF ABSTRACT Unlimited
---	--	---	---

Table of Contents

Cover.....	1
SF 298.....	2
Table of Contents.....	3
Introduction.....	4
Body.....	5-11
Key Research Accomplishments.....	11
Reportable Outcomes.....	11-12
Conclusions.....	12
References.....	N/A
Appendices.....	13-29

INTRODUCTION

Breast cancer is a complex disease whose ultimate understanding will require the integration of facts resulting from a multidisciplinary approach. Continued basic science research will provide a fuller understanding of the basic mechanisms of breast cancer that is necessary to conquer the disease in humans. In order to have the scientific human armamentarium to further this understanding, this training grant focuses on producing qualified scientists for careers as independent investigators in the area of breast cancer. The rationale for a targeted training grant in breast cancer is based on the belief that the elucidation of how oncogenes, tumor suppressor genes, hormones and growth factors act at the molecular level and as developmental-specific agents are critical questions directly relevant to the etiology, prevention, diagnosis, treatment and prognosis of human breast cancer. The training program has drawn together individuals who have an established research and training background in the mammary gland with individuals who have a research and training background in cell biology, molecular endocrinology, molecular biology, molecular virology, viral oncology, molecular genetics and biochemistry. The strength of the program is two-fold. First, the program gathers together members of diverse disciplines to focus on the training of predoctoral and postdoctoral students for careers in an area that, by its biological nature, is multi-disciplinary. Second, the program introduces new intellectual approaches and insights to the problem of breast cancer that will be continued by the next generation of research scientists.

The design of the training program provides for trainees to be exposed to clinical problems and recent advances as well as the multi-disciplinary approaches to answering fundamental questions related to breast cancer research. The familiarity and close proximity of the training faculty facilitates and encourages the development of a new generation of research scientists who will be able to understand the problem of breast cancer at a more complex level and from a multi-disciplinary orientation.

BODYa. Trainees

The goal of this training program is to provide an environment for training in breast cancer research. To foster this goal, candidate graduate students have to meet a minimum set of requirements. Graduate students have to be at least in their second year of graduate school and have selected a thesis problem focusing on an aspect of mammary gland growth, differentiation and/or cancer. These students are supported for two years by the training program provided they maintain satisfactory progress in their research program and they participate in the weekly "Breast" seminar and attend the course "Molecular Carcinogenesis". The two postdoctoral fellows are supported by the training program for two to three years provided they maintain satisfactory progress in their research project and actively participate in the weekly "Breast" seminar. The five fellows from the grant year 2000 - 2001, their departmental affiliation, mentor, research problem and an Abstract of their research is provided below.

b. Research Projects

- 1) Geetika Chakravarty, Ph.D., Department of Molecular and Cellular Biology; Mentor, Jeffrey Rosen, Ph.D., Professor; "p190-B in mammary development and cancer."

ABSTRACT

In addition to systemic hormones, local growth factors, stroma, and the extracellular matrix (ECM), signaling proteins also play a critical role in tissue remodeling during mammary gland development. p190-B is a signaling RhoGTPase activating protein that has been shown to regulate cytoskeletal assembly through Rho proteins. The overall objective of this fellowship was to establish that p190-B expression is critical for ductal morphogenesis and that its aberrant expression facilitates cancer progression.

Since our *in situ* and Northern blots data showed that p190-B expression was higher in the outer cap cell layer of the TEBs, we wanted to determine if loss of p190-B expression would compromise ductal morphogenesis. To address this issue and to establish a direct genetic connection between p190-B expression and the ability of TEBs to invade the fat pad, embryonic mammary buds from neonatal lethal p190-B knockout mice were rescued by transplantation into the cleared mammary fat pad of RAG1^{-/-} mice. We monitored their ability to give rise to the mammary ductal tree. Our hypothesis was that loss of p190-B expression would compromise the ability of TEBs to invade the fat pad and thus their capacity to give rise to the mammary ductal tree. As opposed to the wild type epithelium that repopulated the gland in 75% (12/16) transplants, none (0/5) of the null transplants grew out. The heterozygous mice had an intermediate growth rate with a repopulation rate of 40% (6/15), suggesting that the single functional allele of p190-B was less efficient in facilitating ductal morphogenesis.

As none of the null transplants grew out, our results could be interpreted differently. One could infer that the retarded growth of the null embryonic buds was due to 1) morphologically abnormal mammary buds in E16 embryos, or 2) the null buds were

developmentally retarded at E16 of pregnancy. To address the first issue, ventral skin from wild type and null E16 embryos were fixed and examined under a dissecting scope to visualize distinct embryonic bud morphology. In all the cases studied, we could identify distinct inguinal and thoracic embryonic buds under the scope. To address the second concern, serial sections from wild type, heterozygous and null E16 buds were stained with developmental markers like Lef-1. No apparent differences were noted in the expression of lef-1 in null versus wild type mammary buds suggesting that the buds were developmentally normal. We will determine the viability of the null embryonic buds using *in vitro* organ culture techniques.

In the embryonic transplant studies, only 40% heterozygous embryonic buds were capable of repopulating the gland. We asked the question if one allele of p190-B was sufficient to drive ductal morphogenesis in heterozygous adult virgin females. For these studies, ductal morphogenesis in wild type and heterozygous adult virgin females was compared at 3wks, 4wks, 5wks and 6wks of age. In accordance with our earlier observations, p190-B heterozygous females had significantly retarded ductal growth at 3wks and 4wks time points. However, by six weeks of age this defect could be partially rescued suggesting that indeed a single functional allele of p190-B was less efficient in facilitating ductal morphogenesis in immature virgin females.

In order to better understand how p190-B may be implicated in signaling pathways regulating cell transformation and/or invasion, we had previously transiently transfected p190-B into MCF-10A human mammary epithelial cells using an efficient adenovirus-mediated transfection protocol and measured their adhesive capacities. However, being a transient transfection assay we failed to measure the invasive capacities of these cells. To circumvent this problem, we made stable cultures using retroviral vectors. However, for reasons unknown, we could obtain only two late passage clones that overexpressed p190-B. Studies are in progress to characterize these clones in terms of their growth and migratory potential. We are also generating Tet regulatable p190-B cells to measure their invasive potential under on/off conditions using modified Boyden chamber assay.

In summary, these experiments demonstrate p190-B, a RhoGTPase, is required for normal ductal morphogenesis. Current experiments are examining if p190-B imparts invasive potential to non-invasive human breast tumor cells.

- 2) Xianshu Cui, Ph.D., Department of Molecular Virology and Microbiology; Mentor, Larry Donehower, Ph.D., Associate Professor; "Interactions of wnt-1 and tumor-suppressor genes."

ABSTRACT

During the last year Xian-Shu Cui has been involved in two major projects. The first project involved the characterization of gene expression patterns in mouse mammary tumors in the presence and absence of the tumor suppressor p53. The second project was the analysis of gene expression in hormone-stimulated mammary glands in the presence and absence of p53. Before she completed her postdoctoral training and left the laboratory in May 2001, Xianshu completed many aspects of the first project and made strong progress on the second project. Specifics of her accomplishments are outlined below.

Analysis of gene expression patterns in mouse mammary tumors in the presence and absence of p53: In our laboratory, we have characterized the biological and genetic aspects of mammary tumors arising in our *Wnt-1/p53* mouse mammary tumor model. The *Wnt-1* transgenic mouse contains a *Wnt-1* oncogene driven by a mouse mammary tumor virus long terminal repeat (MMTV LTR) promoter which results in the stochastic appearance of mammary tumors within 3-12 months in the transgenic females. By crossing the *Wnt-1* transgenic mouse to our p53 knockout mouse, we had previously shown that *Wnt-1* TG females null for p53 (p53^{-/-}) developed mammary tumors that arose sooner, grew much more rapidly, and showed more chromosomal instability and less differentiated characteristics than *Wnt-1* TG females with wild type p53 (p53^{+/+}). To identify genes that might be associated with these p53-dependent differences, we performed cDNA microarray analyses (and other types of comparative analyses) on p53^{+/+} and p53^{-/-} *Wnt-1* TG mammary tumors to identify differentially expressed genes. The differentially expressed genes identified in screens were confirmed by Northern and Western blot analyses. As indicated in the accompanying reprint, two categories of differentially expressed genes were identified. The majority of the differentially expressed genes were upregulated in p53^{+/+} tumors. The first group was cell cycle regulatory genes, such as c-kit, p21, and cyclin B1 (decreased in p53^{+/+} tumors). The second group of genes identified were genes often considered differentiation markers, such as cytokeratin 19, alpha smooth muscle actin and kappa casein. The upregulation in the p53^{+/+} tumors is consistent with the more differentiated morphology and less aggressive features of the p53^{+/+} tumors. Thus, while tumors can arise and progress in the presence of functioning wild type p53, p53 may directly or indirectly regulate expression of an array of genes that facilitate differentiation and inhibit proliferation, contributing to a more differentiated, slow growing, and genomically stable phenotype.

Differential gene expression in hormone-stimulated mammary glands in the presence and absence of p53: Xian-Shu has been utilizing cDNA microarray technology to investigate an intriguing mammary gland model. Dr. Medina has shown that transplanted mammary glands from p53^{-/-} females are highly sensitive to mammary tumorigenesis, particularly when stimulated with hormones and/or carcinogens. Moreover, he has found that mammary epithelial cells in the normal p53^{-/-} mammary glands exhibit a high degree of chromosomal instability when stimulated by estrogen and progesterone or merely progesterone by itself. Normal p53^{+/+} mammary glands are not susceptible to this hormone-induced chromosomal instability. To better understand the mechanisms behind this chromosomal instability, we prepared mRNA from hormone stimulated p53^{-/-} and p53^{+/+} mammary epithelial cells and compared their gene expression patterns by microarray analyses repeated at least three times. Initial screens revealing a number of differentially expressed genes and these are beginning to be further analyzed in an attempt to identify the most biologically relevant genes.

- 3) Fabrice Petit, Ph.D., Department of Molecular and Cellular Biology; Mentor, Sophis Tsai, Ph.D., Professor; "Role of COUP-TFII in mammary gland development and tumorigenesis."

ABSTRACT

COUP-TFs (Chicken Ovalbumin Upstream Promoter-Transcription Factors) are orphan members of the steroid/thyroid hormone receptor superfamily. In mouse, two COUP-TF

members have been isolated, COUP-TFI and COUP-TFII. COUP-TFI is highly expressed in the central nervous system and peripheral nervous system, while COUP-TFII is highly expressed in mesenchymal cells during organogenesis. To study the physiological function of COUP-TFII *in vivo*, we have generated null mice for this gene. The mutant mice die during the early embryonic development around E10 days of gestation from heart and vasculature defects. It has been shown that Angiopoietin-1 (Ang1), a potent angiogenic factor, is down-regulated in COUP-TFII null mice. Interestingly, COUP-TFII is highly expressed in mammary gland and in many breast cancer cell lines. So far, no physiological role has been described for COUP-TFII in this organ. Nevertheless, it has been reported that COUP-TFII can either inhibit or enhance the transactivation function of transcription factors such as ER, through a direct interaction. It is possible that COUP-TFII may play a role in the development and/or the function of the mammary gland. Since COUP-TFII null mutants show defects in angiogenesis, which plays key roles in tumor growth and metastasis, it is possible that COUP-TFII plays a role in breast cancer. For these reasons, my project is to use COUP-TFII null mutants to study its role in the mammary gland development and the breast cancer formation. Since the COUP-TFII null mice die prior to mammary gland formation, it does not allow us to analyze the physiological function of COUP-TFII during organogenesis. To bypass the early lethality, we decided to rescue the null mutants from the angiogenesis and heart defects. Ang1 is expressed in the mesenchymal cells surrounding the endothelial cells and its deletion in mouse results in defects in vascular and heart development, similar to those observed in COUP-TFII null mutants. In addition, we have shown that Ang1 is down regulated in COUP-TFII mutants and it is a direct target of COUP-TFII. Therefore, Ang1 is likely to mediate all or part of COUP-TFII function in vascular system.

To rescue the COUP-TFII null mutant lethality, we used the Ang1 promoter to drive the expression of COUP-TFII. A fragment of 10.5 kb of the angiopoietin-1 gene was cloned from a Bacterial Artificial Chromosome (BAC) and used to specifically knock in the endogenous Ang1 gene. For this purpose, a first construct containing the COUP-TFII cDNA with its own first intron, the neomycin gene floxed by loxP sites has been made and inserted into the first exon of Ang1 gene. The final construct has been electroporated into Embryonic Stem (ES) cells isolated from the strain mouse 129. After screening of 329 ES clones resistant to G418 (neomycin resistance), 9 clones were positive for the Ang1-COUP-TFII construct. These clones have been injected into blastocysts isolated from a C57BL/6 mouse mother. The injected blastocysts have been transferred to a foster SWISS mouse. From this transfer, 5 chimera C57BL/6-129 were born and crossed with C57BL/6 mice to check whether a germ line transmission occurs. The analysis of the new born mice have shown that 2 lines are heterozygotes for the knock-in construct and can transmit it to their descendants. We are in the process of getting the first double heterozygotes for COUP-TFII and Ang1-COUP-TFII knock-in. After generation of these mice, we will mate them with COUP-TFII heterozygous mice in order to get the first COUP-TFII null mice expressing COUP-TFII under the influence of Ang1 promoter. Therefore, the expression of COUP-TFII in the vascular system should rescue the embryonic lethality and allow us to examine the role of COUP-TFII in mammary gland development and tumor progression. Before analyzing these knock-in mice, we need to know precisely when and where COUP-TFII is expressed during mammary gland development. Using *in situ* hybridization techniques and COUP-TFII-LacZ knock in mice, we are currently analyzing the detailed expression patterns of COUP-TFII in mammary gland.

- 4) Yue Wei, Department of Biochemistry; Mentor, Wade Harper, Ph.D., Professor; "Molecular dissection of the S-phase transcriptional program controlled by the cyclin E/p220^{NPAT} signaling pathway."

ABSTRACT

Deregulation of cell cycle pathways is a common occurrence in the development of neoplasia. In breast cancer, deregulation of the cyclin E/Cdk2 pathway is frequently seen and both cyclin E and its negative regulator p27 are independent prognostic markers for breast cancer. Although much is known about how cyclin E/Cdk2 is regulated, relatively little is known concerning how this kinase brings about duplication of the genome. Our lab, together with the Harlow lab, has uncovered a novel transcriptional regulatory pathway control by cyclin E/Cdk2, which may be responsible for mediating critical events in S-phase, including induction of histone gene transcription. The link between cyclin E and an S phase transcriptional program is made by the cyclin E/Cdk2 substrate p220^{NPAT}. p220 localizes in cell cycle regulated nuclear foci that are co-incident with Cajal Bodies (CBs). p220 foci are tethered to histone gene clusters on chromosomes 6p21 and 1q21. Overexpression of p220 increases transcription from histone promoter reporters, and this activation requires cyclin E/Cdk2 mediated p220 phosphorylation. Ectopic p220 expression accelerates S-phase entry and there is evidence that p220 is rate limiting for cell division. How p220 controls essential S-phases processes is unknown.

Two aims were examined over the past year. First, we analyzed the role of p220^{NPAT} in the coordinate activation of endogenous histone genes. Second, we examined the transcriptional regulation of non-histone genes by p220^{NPAT}. These experiments demonstrated that p220^{NPAT} promotes histone promoter reporter gene transcription in synchronized cell. Previous work showed that overexpression of p220 promoted the transcription of reporter gene (luciferase) from histone promoters in cycling 293T and U2OS cells. Since overexpression of p220 also accelerates the entry of S phase, it is not clear whether the transcription activation of the reporter gene is due to p220 activity or due to the activation of S phase entry. The recent experiments indicated that in U2OS cells synchronized by nocodazole in G2 phase and released into G1 phase, overexpression of p220 still can promote the transcription from histone promoters, which suggests that p220 itself may have the transcription activation to histone promoter.

I have established cell lines using a doxycyclin-inducible Tet-ON system in U2OS cells, which provides for extremely low levels of expression in the absence of inducing agent. The construction of the Tet-ON p220 cells involves multiple steps. I have thus far screened ~300 colonies for expression and have identified several clones that give inducible p220 expression by immunoblotting with a consequent increase in the number of S-phase cells in the culture.

A loss-of-function approach addresses whether p220 is required for histone gene transcription. My work focuses on the use of siRNAs (small interference RNA) to ablate p220 expression. This approach takes advantage of a 21-bp double-stranded RNA (dsRNA) oligo that is homologous to a sequence in the target gene and effectively silences expression through post-transcriptional and/or transcriptional mechanisms. Two pairs of oligonucleotides have been tried, and preliminary data showed that both of them could inhibit the expression of p220 in U2OS cells and the induced overexpression of p220 in U2OSTetONp220 cells, while one of

them was more effective than the other. The effects on cell cycle progression and histone transcription will be assessed in future experiments.

- 5) Michelle Martin, Baylor Breast Center, Department of Molecular and Cellular Biology; Mentor, Peter O'Connell, Ph.D., Professor; "The metastasis gene on chromosome 14q."

ABSTRACT

This project involves the characterization of a region of chromosome 14q in breast cancer. Unlike many markers tested as LOH, the loss of marker D14S62, which lies in this region, was associated with node-negative disease and slower spread to distant sites. A physical map of this region was completed that included 3 YACs and approximately 90 promising EST clones. Mapping of MTA1 (metastasis associated 1) showed that it mapped to YAC 859D4, which was inside our region of interest. We also have mapped MTA1 to BAC 76E12, which has been sequenced and confirmed to map onto YAC 849D4

Construction of a physical was completed using YACs and ESTs to completely define the region of interest on chromosome 14q31.2, plus the surrounding area on chromosome 14q. The completed map contained a minimum tiling path of three YAC clones, 755C2, 772E4, and 859D4 that spanned the region. Next, an EST-based map of the region was constructed that included approximately 90 ESTs of known and unknown identity. These ESTs covered both the D14S62 region and regions both proximal and distal to insure complete coverage of the area. The locations of the ESTs in the D14S62 region were verified by mapping onto the above YACs.

90 ESTs chosen for the mapping strategy and were arrayed as probes onto nytran filters in duplicate, then interrogated with radiolabeled cDNA from a variety of breast cancer cell lines such as MDA-468, MDA-MB-435, and MCF-10A. Differences of expression in the ESTs in cells of differing metastatic potential helped to prioritize these genes as either breast epithelial expressed or potential candidate metastasis-related genes. Also, we determined the MTA1 gene was a promising candidate through database mining and additional mapping studies. MTA1 was confirmed to map onto YAC 859D4 and BAC 76E12, which had been sequenced and confirmed to map onto 859D4.

Current experiments involve the characterization of candidate gene MTA1 by *in situ* hybridization, immunohistochemistry, and western blot analysis of primary node-negative and primary node-positive human breast tumors. A full-length construct of MTA1 with a T7 tag was obtained from Dr. Rakesh Kumar from MD Anderson Cancer Center. This clone is being used as a positive control to determine with certainty which band on the gel corresponds to MTA1. A monoclonal antibody to the T7 tag was also purchased from Novagen to assist in the identification of the MTA1-specific band. Once the identity of the MTA1 band is known, western blot analysis of twenty tumors from the Breast Center dead-end bank will begin. These results will be analyzed and used to determine how large a sample size will be needed to achieve statistical significance.

Immunohistochemistry is also being performed on tissue arrays that contain samples of various normal tissues including endometrium, prostate, tonsil, appendix, kidney,

breast, and others. Differential patterns of expression have been observed, and work is under way now to make certain the signal is MTA1-specific before proceeding to breast cancer samples.

KEY RESEARCH ACCOMPLISHMENTS

The major results of the past year in bullet form are:

- P190-B, a RhoGTPase, is required for normal mammary morphogenesis.
- CDNA array analysis of p53^{+/+} versus P53^{-/-} mammary tumors revealed the down regulation of several genes associated with morphological differentiation and less aggressive growth in p53^{-/-} tumors.
- COUP-II has been knocked into the Ang1 locus. Using such mice, the embryonic lethality of COUP-II is rescued providing a model system to examine the function of COUP-II in the mammary gland.
- The cyclin E/CDK2 substrate p220^{NPAT} promotes histone promoter gene transcription.
- The putative metastatic gene, MTA1, has been physically mapped on YAC859D4 and BAC76E12.

REPORTABLE OUTCOMES

Enhancement Programs

Three education programs specific for this training program were functional over the past year. The weekly "Breast" seminar included faculty and trainees. The schedule for the seminar series is shown in Table 1.

The second education enhancement program is the Invited Speakers program. This program allows both the faculty and fellows supported by the program to interact with the invited speaker. The two speakers were Dr. Sara Sukumar who spoke on the subject of utilization of array technologies to breast cancer studies and Dr. Lewis Chodosh who spoke on the subject of transgenic mouse models for breast cancer.

The third education enhancement program is the course in "Molecular Carcinogenesis," which is given every Winter bloc and each predoctoral trainee is required to pass. This course is organized by Dr. Larry Donehower and the teaching faculty includes Drs. Medina, Harper, Donehower and Brown.

Trainee Review

With respect to trainee review, there are two turnovers for the new year. Yue He left the Ph.D. program for personal reasons in late August, 2000. This position was not refilled due to

the lack of suitable candidates in the already started academic year. Xianshu Cui finished her postdoctoral studies and departed Baylor College of Medicine to pursue opportunities in the biotechnology industry in California. The prospective trainees to fill the two vacated positions were nominated by letter and supporting documentation and the successful applicants notified by letter that their respective fellowships would start July 1, 2001.

Publications

Three of the supported trainees have publications in leading scientific journals. These are listed below and are provided as appendices.

1. Cui, X.-S. and Donehower, L.A. Differential gene expression in mouse mammary adenocarcinomas in the presence and absence of wild type p53. *Oncogene* 19:5988-5996, 2000.
2. Ma, T., Van Tine, B.A., Wei, Y., Garrett, M.D., Nelson, D., Adams, P.D., Wang, J., Qin, J., Chow, L.T., and Harper, J.W. Cell cycle-regulated phosphorylation of p220^{NPAT} by cyclin E/Cdk2 in Cajal bodies promotes histone gene transcription. *Genes & Development* 14:2298-2313, 2000.
3. Martin, M.D., Fischbach, K., Osborne, C.K., Mohsin, S.K., Allred, D.C., and O'Connell, P. Loss of heterozygosity events impeding breast cancer metastasis contain the *MTA1* gene. *Cancer Res* 61:3578-3580, 2001.

FLOOD LOSSES

The flood due to Tropical Storm Allison seriously affected the research program of one of our trainees. Dr. Geetika Chakravarty lost approximately 100 mice that were heterozygous for p190-B and reagents worth \$6154.00. This has set her back in experiments by a year as the mice are difficult to breed. Moreover, it will take some time to obtain fresh reagents to carryout the experiments from scratch.

CONCLUSIONS

The training program in breast cancer is functioning as planned and major alterations are not planned at this time. The inclusion of faculty from the Baylor Breast Center as participating faculty has added a translational dimension.

APPENDICES

Table 1.
Publications.

Table 1
Breast Disease Research Group
2000-2001 Schedule
Wednesdays 12:00 p.m., Room M616 (Debakey Bldg.)

DATE	NAME	TITLE	DEPARTMENT
09/13	Saraswati Sukumar, Ph.D.	Associate Professor	Johns Hopkins Univ.
09/20	Daniel Medina, Ph.D.	Professor	Mol. & Cellular Biology
09/27	Britt Glaunsinger	Graduate Student	Molecular Virology
10/04	No talk		
10/11	Richard M. Elledge, Ph.D. Gary M. Clark, Ph.D.	Associate Professor Professor	Breast Center
10/18	No talk		
10/25	Khandan Keyomarsi, Ph.D.	Associate Professor	MD Anderson - Houston
11/01	C. Marcelo Aldaz, M.D.	Associate Professor	MD Anderson - Smithville
11/08	Guillermina (Gigi) Lozano, Ph.D.	Molecular Genetics	MD Anderson - Houston
11/15	No talk		
11/22	Holiday		
11/29	Torsten Hopp, Ph.D.	Instructor	Breast Center
12/06	No talk		
12/13	Darryl Hadsell, Ph.D.	Assistant Professor	Nutrition – CNRC
12/20	No talk		
12/27	Holiday		
01/03	No talk		
01/10	Geetika Chakravarty, Ph.D.	Postdoctoral Associate	Mol. & Cellular Biology
01/17	Sharon Bonnette, Ph.D.	Postdoctoral Fellow	Nutrition - CNRC
01/24	Salmon Hyder, Ph.D.	Associate Professor	UT Medical School
01/31	John Lydon, Ph.D.	Assistant Professor	Mol. & Cellular Biology
02/07	Steven Townson, Ph.D.	Postdoctoral Associate	Breast Center
02/14	Rachel Schiff, Ph.D.	Instructor	Breast Center
02/21	No talk		
02/28	Thea Goepfert, Ph.D.	Postdoctoral Assoc.	Mol. & Cellular Biology
03/07	Rescheduled Dr. Chodosh	Assistant Professor	Univ. of Pennsylvania
03/14	No talk		
03/21	Ming Zhang, Ph.D. (Lab)	Assistant Professor	Mol. & Cellular Biology
03/28	No talk		
04/04	Harold R. Garner, Ph.D.	Professor	UT SW Med Ctr., Dallas
04/11	Easter Week		
04/18	Lynn M. Matrisian, Ph.D.	Professor	Vanderbilt Univ.
04/25	Lewis Chodosh, Ph.D.	Assistant Professor.	Univ. of Pennsylvania
05/02	No talk		
05/09	Xiaojiang Cui, Ph.D.	Postdoctoral Fellow	Breast Center
05/16	Rafael Herrera, Ph.D.	Assistant Professor	Breast Center
05/23	No talk		



Differential gene expression in mouse mammary adenocarcinomas in the presence and absence of wild type p53

Xian-Shu Cui¹ and Lawrence A Donehower^{*1,2}

¹Department of Molecular Virology and Microbiology, Baylor College of Medicine, Houston, Texas, TX 77030, USA;

²Department of Molecular and Cellular Biology, Baylor College of Medicine, Houston, Texas, TX 77030, USA

The tumor suppressor p53 transcriptionally regulates a large number of target genes that may affect cell growth and cell death pathways. To better understand the role of p53 loss in tumorigenesis, we have developed a mouse mammary cancer model, the *Wnt-1* TG/p53 model. *Wnt-1* transgenic females that are p53^{-/-} develop mammary adenocarcinomas that arise sooner, grow faster, appear more anaplastic, and have higher levels of chromosomal instability than their *Wnt-1* transgenic p53^{+/+} counterparts. In this study, we used several assays to determine whether the presence or absence of p53 affects gene expression patterns in the mammary adenocarcinomas. Most of the differentially expressed genes are increased in p53^{+/+} tumors and many of these represent known target genes of p53 (p21^{WAF1/CIP1}, cyclin G1, alpha smooth muscle actin, and cytokeratin 19). Some of these genes (cytokeratin 19, alpha smooth muscle actin, and kappa casein) represent mammary gland differentiation markers which may contribute to the inhibited tumor progression and are consistent with the more differentiated histopathology observed in the p53^{+/+} tumors. Several differentially expressed genes are growth regulatory in function (p21, *c-kit*, and cyclin B1) and their altered expression levels correlate well with the differing growth properties of the p53^{+/+} and p53^{-/-} tumors. Thus, while tumors can arise and progress in the presence of functioning wild type p53, p53 may directly or indirectly regulate expression of an array of genes that facilitate differentiation and inhibit proliferation, contributing to a more differentiated, slow growing, and genomically stable phenotype. *Oncogene* (2000) 19, 5988–5996.

Keywords: p53; mouse mammary tumor; *Wnt-1*; p21^{WAF1/CIP1}; *c-kit*; cyclin B1

Introduction

The p53 tumor suppressor gene is lost or mutated in over half of all human cancers (Levine, 1997; Lozano and Elledge, 2000). In addition, inactivation of p53 function without loss of p53 structural integrity may occur by a number of different mechanisms (Moll and Schramm 1998; Freedman *et al.*, 1999). Nevertheless, a significant fraction of human tumors arise and progress

without incurring mutation or functional loss of p53 activity. In such tumors, retention of p53 activity has important clinical consequences. These tumors often have better prognoses and better responses to chemotherapeutic regimens (Kirsch and Kastan, 1998; Wallace-Brodeur and Lowe, 1999). Moreover, some tumor types with intact p53 exhibit less anaplastic histopathology, lower proliferation levels, and less chromosomal instability (Donehower, 1996).

The p53 protein is a transcriptional regulatory factor that responds to a number of cellular stresses, including DNA damage and activated cellular oncogenes (Giaccia and Kastan, 1998). The activated p53 protein can transactivate a number of genes involved either in cell cycle control or in cell apoptosis pathways (el-Deiry, 1998). One of the first identified targets of p53 was the p21^{WAF1/CIP1} cyclin-dependent kinase inhibitor, which directly interacts with G1 cyclin-cdk complexes and inhibits their activity, and thus is an important component of the p53-mediated G1 arrest checkpoint (el-Deiry *et al.*, 1993; Harper *et al.*, 1993). Another important p53 target relevant to the apoptotic function of p53 is bax, a pro-apoptotic protein (Miyashita and Reed, 1995). Recently, the introduction of large scale screening technologies has greatly increased the number of known p53 targets. Using techniques such as serial analysis of gene expression (SAGE) and cDNA array analyses, a library of genes have been assembled that are either upregulated or downregulated by p53 (Polyak *et al.*, 1997; Yu *et al.*, 1999; Zhao *et al.*, 2000). Some of these genes regulate cell growth or death control, but others appear to be involved in physiological processes not directly related to growth or death (Polyak *et al.*, 1997; Zhao *et al.*, 2000). Moreover, there is a great deal of heterogeneity in the response of p53 target genes. A number of factors influence the types of p53-responsive genes that are activated or repressed, including p53 levels, the nature of the cellular stress, and the cell type being studied (Yu *et al.*, 1999; Zhao *et al.*, 2000).

While the SAGE and cDNA array screens have provided powerful tools for the identification of novel p53 target genes, there are potential limitations in the use of such screens. Generally, very high levels of p53 are often produced, which may fail to identify target genes regulated by physiological levels of p53. In addition, cancer cell lines of various types are often used and these cells have other genetic defects which may prevent identification of bona fide p53 targets. Finally, the experiments are performed in cell culture, and so targets may be missed that result from the activation of p53 in its normal *in-vivo* context.

*Correspondence: LA Donehower, Department of Molecular Virology and Microbiology, Baylor College of Medicine, One Baylor Plaza, Houston, TX 77030, USA
Received 26 June 2000; revised 28 September 2000; accepted 4 October 2000

To circumvent some of these potential limitations and identify genes regulated by p53 *in vivo* which might be directly relevant to tumorigenesis, we have utilized a murine mammary cancer model, the *Wnt-1* TG/p53 mouse. *Wnt-1* TG mice contain several copies of a germline *Wnt-1* oncogene driven by a mammary gland specific mouse mammary tumor virus promoter (Tsukamoto *et al.*, 1988). The female *Wnt-1* transgenic mice develop early mammary gland hyperplasia and usually succumb to mammary adenocarcinomas between the ages of 3 and 12 months. In order to determine the effects of p53 dosage on mammary tumorigenesis in this model, we crossed the *Wnt-1* TG mice to p53-deficient mice and the *Wnt-1* transgenic female offspring were monitored for mammary tumors in the presence and absence of p53 (Donehower *et al.*, 1995). As shown in Table 1, the absence of p53 (p53^{-/-}) in the presence of the *Wnt-1* transgene resulted in mammary tumors that appeared sooner, grew faster, displayed less differentiated and more anaplastic histopathology, and exhibited more chromosomal instability than their *Wnt-1* TG p53^{+/+} counterparts (Donehower *et al.*, 1995; Jones *et al.*, 1997). Moreover, these differences in tumorigenic phenotypes were likely to be due directly to p53 status, since the p53 gene was not mutated or suppressed in the p53^{+/+} tumors (Donehower *et al.*, 1995).

Because the p53^{+/+} and p53^{-/-} *Wnt-1* TG mice generate the same type of mammary adenocarcinomas, we decided to compare their gene expression patterns on the hypothesis that differences in gene expression might be relevant to p53 status and the observed tumorigenic phenotypes. While we believe there are a number of advantages of our *in-vivo* tumorigenesis model (e.g. a closer approximation to real physiological conditions), there may also be at least three potential limitations not encountered in the *in-vitro* screens. First, mammary tumors are heterogeneous and not composed solely of tumor cells. They are a

mixture of epithelial tumor cells, myoepithelial and stromal components, adipose cells, and blood vessels. However, we have found that the epithelial tumor component usually predominates and thus the other nontumor components should not obscure any strong differences in gene expression. Second, despite being of identical histopathological type, intertumoral variation may be significant and apparent differences might be due to such variation rather than p53 status. To address this problem we analysed expression patterns in five to eight different tumors of each p53 genotype. Thus, if all or almost all p53^{+/+} tumors show higher expression levels of a particular gene than is seen in their p53^{-/-} counterparts, then this difference is likely to be significant. Finally, comparison of end stage p53^{+/+} and p53^{-/-} tumors will not necessarily identify direct p53 targets. Instead, secondary p53 targets or genes altered in expression due to other genetic changes might be detected. The discovery that many of the differentially regulated genes in our tumor model are known p53 target genes has reassured us that, in many cases, the differential expression is likely to be due directly to p53 expression levels.

Using several different approaches, we show here that, in addition to altering biological and genetic properties of mammary adenocarcinomas, p53 status affects gene expression patterns. At least seven differentially expressed genes have been identified in comparing p53^{+/+} and p53^{-/-} tumors (Table 2). Some of the differentially expressed genes are clearly related to growth control, while others appear to be differentiation markers. The observed differential expression patterns of particular genes fit well with the biological properties of the parental tumors, suggesting that these genes may be a cause rather than an effect of the tumor phenotype. Thus, these results may provide further insights into the role of p53 target genes in the pleiotropic biological effects associated with tumorigenesis.

Table 1 Biological and genetic properties of *Wnt-1* TG p53^{+/+} and *Wnt-1* TG p53^{-/-} mammary adenocarcinomas

Property	p53 ^{+/+}	p53 ^{-/-}
Tumor type	Mammary adenocarcinoma	Mammary adenocarcinoma
50% tumor incidence	22.5 weeks	11.5 weeks
100% tumor incidence	40 weeks	15 weeks
Mean tumor growth rate	800 cu. mm/wk	3400 cu. mm/wk
Mean percentage of mitotic tumor cells	0.0027	0.0070
Mean percentage of apoptotic tumor cells	0.32	0.48
Percentage of tumors with abnormal chromosomes	33	100
Mean number of abnormal chromosomes per tumor	0.3	1.7
Histopathological appearance	Uniform nuclei, differentiated, more stroma	Anaplastic, undifferentiated, less stroma

Table 2 Differentially expressed genes in *Wnt-1* TG p53^{+/+} and *Wnt-1* TG p53^{-/-} mammary adenocarcinomas

Gene	ID method	p53 ^{+/+} levels	Mean difference	P-value	Protein	p53 target	Function/Marker
Alpha smooth muscle actin	Diff. Display	Increased	4.25	<0.001	Yes	Yes	Myoepithelial marker
Kappa casein	Diff. Display	Increased	3.18	0.045	ND	No	Luminal cell epithelial marker
<i>c-kit</i>	cDNA Array	Increased	2.38	0.01	Yes	No	Receptor tyrosine kinase
Cytokeratin 19	cDNA Array	Increased	2.73	0.003	Yes	Yes	Epithelial cell intermediate filament marker
P21 ^{WAF1/CIP1}	Northern	Increased	2.27	0.01	ND	Yes	Cdk inhibitor, growth marker
Cyclin B1	RNAse Prot	Decreased	2.31	0.04	Yes	Yes	Mitotic cyclin, growth marker
Cyclin G1	RNAse Prot	Increased	1.79	0.04	Yes	Yes	Function unclear poss. growth marker

Results

Differentially expressed genes identified by differential display PCR

To identify differentially expressed genes in *Wnt-1* TG p53^{+/+} and *Wnt-1* TG p53^{-/-} tumors, we utilized several different types of screening methods. RNA differential display and cDNA array methods were used to randomly screen the tumors for differentially expressed genes. In addition, Northern blot and RNase protection assays were employed to investigate specific known candidate genes. Each of these approaches revealed differentially expressed genes. Our first set of experiments employed RNA differential display PCR to screen tumor RNAs from *Wnt-1* TG p53^{+/+}, *Wnt-1* TG p53^{+/-} LOH, and *Wnt-1* TG p53^{-/-} tumors (Liang and Pardee, 1992). The *Wnt-1* TG p53^{+/-} LOH tumors are null for p53 because the remaining p53 wild type allele has been deleted during mammary tumorigenesis (Donehower *et al.*, 1995). A number of candidate fragments were identified by this PCR-based method. An example of a fragment specific for the p53^{+/+} tumor RNAs is shown in Figure 1a. All fragments identified in this assay were at increased levels in the p53^{+/+} tumors. These p53^{+/+} specific fragments were then excised from the gel, reamplified with the appropriate differential display primers, labeled with ³²P and used as probes on Northern blots containing total RNAs from five p53^{+/+} and five p53^{-/-} tumors. Two separate differential display

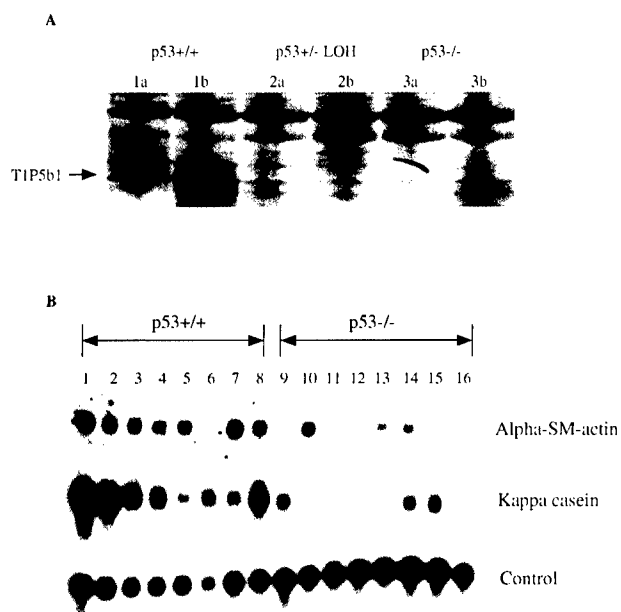


Figure 1 Differentially expressed genes in *Wnt-1* TG p53^{+/+} mice and *Wnt-1* TG p53^{-/-} mice identified by differential display PCR and confirmed by Northern blot hybridization. (a) A representative differential display PCR product (TIP5b1, arrow) expressed at higher levels in the *Wnt-1* TG p53^{+/+} tumors compared to either *Wnt-1* TG p53^{+/-} LOH or *Wnt-1* TG p53^{-/-} tumors. (b) Northern blot results of two genes (alpha smooth muscle actin and kappa casein). Eight different tumor RNA samples from each *Wnt-1* TG genotype (p53^{+/+} and p53^{-/-}) were loaded. After normalizing to the control RNA (GAPDH) signal, significant increases in RNA levels of these two genes are observed in *Wnt-1* TG p53^{+/+} tumors

fragments consistently showed higher hybridization levels in the five p53^{+/+} tumors. These fragments were cloned and sequenced. The sequences were then compared with the GenBank database and were shown to be identical to two murine genes: alpha smooth muscle actin and kappa casein. The murine cDNA sequences of these two genes were then obtained and used to probe a Northern blot containing total RNAs from eight p53^{+/+} mammary adenocarcinomas and eight p53^{-/-} adenocarcinomas (Figure 1b). Note that while there is heterogeneity in the RNA levels of each gene from tumor to tumor, when the hybridization levels are quantitated and normalized to control probe (GAPDH) hybridization intensity, significant increases in RNA levels of these genes are observed in p53^{+/+} tumors. Alpha smooth muscle actin RNA levels were on average 4.2-fold higher in p53^{+/+} tumors compared to p53^{-/-} tumors. Kappa casein had a mean increase of 3.2-fold compared to p53^{-/-} tumors. These differences were significant at the 0.05 level as measured by *t*-test.

Differentially expressed genes identified by cDNA array analysis

As an adjunct to the differential display analyses, we probed array filters containing 588 murine cDNAs (from Clontech) with ³²P-labeled cDNA probes prepared from mRNA derived from either p53^{+/+} or p53^{-/-} tumors. There were two genes that consistently showed differential expression by this method: *c-kit* and cytokeratin 19 (Figure 2a). Both genes showed higher levels of hybridization in the p53^{+/+} tumors. cDNAs from cytokeratin 19 and *c-kit* were labeled with ³²P and hybridized to Northern blots containing mRNAs from multiple p53^{+/+} and p53^{-/-} tumors. Again, while there was considerable heterogeneity in expression levels, the *c-kit* and cytokeratin 19 genes averaged 2.4- and 2.7-fold increases in expression in p53^{+/+} tumors compared to p53^{-/-} tumors (Figure 2b and data not shown). These differences were found to be significant by *t*-test.

Examination of known p53 target genes

Those p53 target genes known to regulate growth control were obvious candidates for analysis. The prototype p53 target gene is p21^{WAF1/CIP1}, a cyclin-dependent kinase inhibitor (el-Deiry *et al.*, 1993; Harper *et al.*, 1993). Northern blot analysis of p53^{+/+} and p53^{-/-} tumor RNAs using a murine p21^{WAF1/CIP1} cDNA probe revealed that the p53^{+/+} tumors averaged 2.3-fold higher levels of p21 compared to the p53^{-/-} tumors (Figure 2c), consistent with the reduced growth rates observed in the p53^{+/+} tumors. These differences were shown to be statistically significant.

Other important cell cycle regulatory proteins are the cyclins. At least two of these, cyclin B1 and cyclin G1, have been shown to be regulated by p53 (Innocente *et al.*, 1999; Taylor *et al.*, 1999; Okamoto and Beach, 1994). Cyclin B1 appears to be directly repressed by p53 and cyclin G1 has been shown to be upregulated by wild type p53. The cyclin mRNA levels were assessed in p53^{+/+} and p53^{-/-} tumors by RNase protection assay using kits specific for murine cyclin

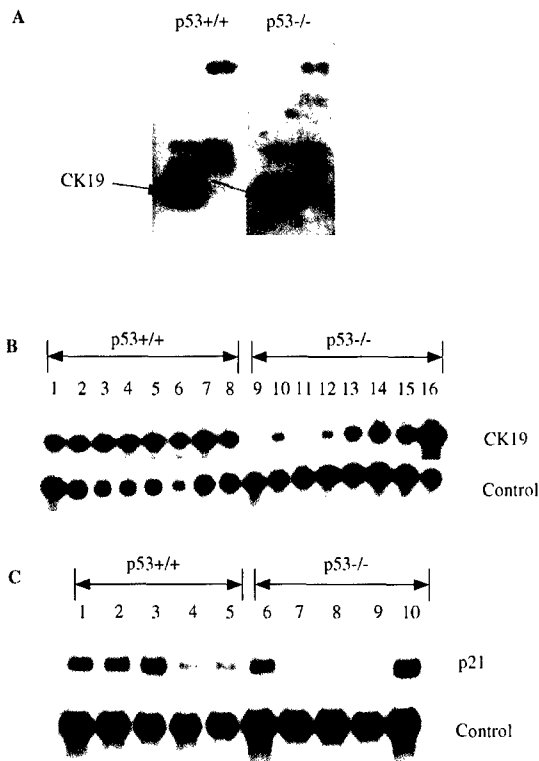


Figure 2 Differentially expressed genes in *Wnt-1* TG p53^{+/+} and *Wnt-1* TG p53^{-/-} mammary tumors identified by cDNA array analysis and candidate gene Northern blot analyses. (a) Representative array showing a strong signal for cytokeratin 19 (CK19) in the *Wnt-1* TG p53^{+/+} sample compared to the *Wnt-1* TG p53^{-/-} sample. (b) Northern blot hybridization of cytokeratin 19 (CK19) with eight tumor samples from each *Wnt-1* TG p53 genotype. After normalization of hybridization signals to control RNA (GAPDH) signals, CK19 expression is significantly higher on average in *Wnt-1* TG p53^{+/+} tumors. (c) Differential expression of the p53-target gene, p21^{WAF1/CIP1}, in *Wnt-1* TG p53^{+/+} and *Wnt-1* TG p53^{-/-} mammary tumors. Northern blot hybridization shows five tumor RNA samples from each p53 genotype loaded for comparison. After normalizing to control (GAPDH) mRNA levels, p21^{WAF1/CIP1} shows significantly higher expression in *Wnt-1* TG p53^{+/+} tumors than in *Wnt-1* TG p53^{-/-} tumors

mRNAs. Interestingly, the only cyclins to show significant differential expression after normalization to the GAPDH control RNA were cyclin B1 and cyclin G1 (data not shown). The p53^{-/-} tumors averaged 2.3-fold higher cyclin B1 than p53^{+/+} tumors and p53^{+/+} tumors showed 1.8-fold elevated levels of cyclin G1 compared to p53^{-/-} tumors. Again, these differences were found to be significant by *t*-test.

Differential protein expression levels

To correlate protein expression levels with the differentially expressed RNAs in the tumors, we performed Western blot analyses on extracts from p53^{+/+} and p53^{-/-} tumors. Figure 3a shows that all of the p53^{+/+} tumors show high levels of alpha smooth muscle actin while only one of the six p53^{-/-} tumors shows comparably high protein levels. Likewise, c-kit and cytokeratin 19 protein levels were generally higher in the p53^{+/+} tumors than their p53^{-/-} counterparts, consistent with the earlier RNA results (Figure 3b). p53^{+/+} tumors also showed higher levels of cyclin G1 than p53^{-/-} tumors

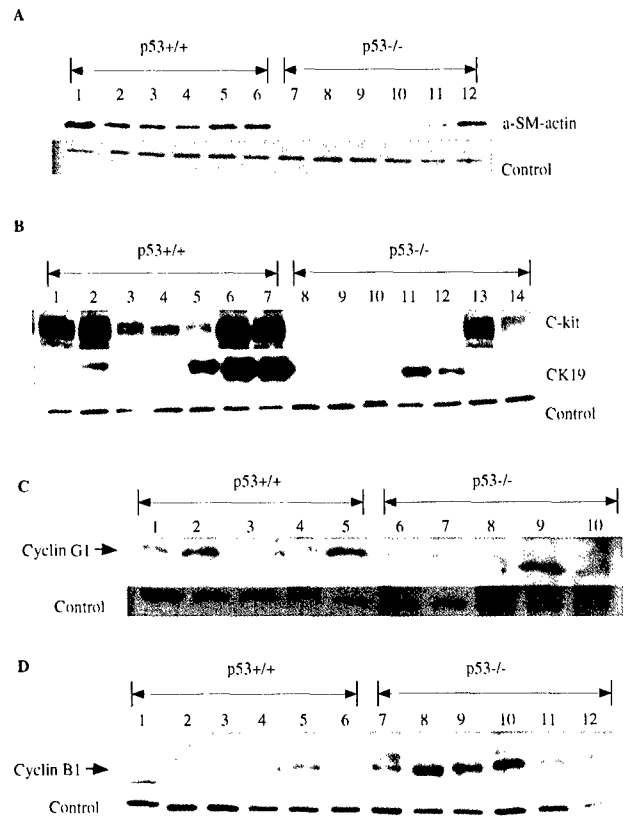


Figure 3 Differential expression of proteins in *Wnt-1* TG p53^{+/+} and *Wnt-1* TG p53^{-/-} mammary tumors as assayed by Western blot analyses. Tumor lysates were subjected to SDS-polyacrylamide gel electrophoresis, followed by transfer to nylon membranes and immunoblotting with antibodies to the various differentially expressed proteins. Each blot was then stripped and immunoblotted with an antibody to vertebrate actin, which served as a loading control. (a) Alpha smooth muscle actin protein expression in six *Wnt-1* TG p53^{+/+} and six *Wnt-1* TG p53^{-/-} mammary tumor lysates. Alpha smooth muscle actin levels were elevated in *Wnt-1* TG p53^{+/+} tumors compared to *Wnt-1* TG p53^{-/-} tumors. (b) c-kit and cytokeratin 19 (CK19) proteins in seven *Wnt-1* TG p53^{+/+} and seven *Wnt-1* TG p53^{-/-} mammary tumor lysates. The *Wnt-1* TG p53^{+/+} tumors had higher levels of c-kit and CK19 proteins on average compared to their *Wnt-1* TG p53^{-/-} counterparts. (c) Cyclin G1 levels in five *Wnt-1* TG p53^{+/+} and five *Wnt-1* TG p53^{-/-} mammary tumor lysates. *Wnt-1* TG p53^{+/+} tumors exhibited higher mean levels of cyclin G1 than *Wnt-1* TG p53^{-/-} tumors. (d) Cyclin B1 protein levels in six *Wnt-1* TG p53^{+/+} and six *Wnt-1* TG p53^{-/-} mammary tumor lysates. *Wnt-1* TG p53^{-/-} tumors exhibited higher mean levels of cyclin B1 than *Wnt-1* TG p53^{+/+} tumors

(Figure 3c). Finally, cyclin B1 protein levels were higher in the majority of p53^{-/-} tumors than in p53^{+/+} tumors (Figure 3d), again correlating well with the RNA data for this gene.

Immunohistochemistry on tumor sections

The high expression of alpha smooth muscle actin in the p53^{+/+} tumors was of interest because this protein is known to be an important marker for the myoepithelial compartment of the mammary gland (Gugliotta *et al.*, 1988). To confirm whether the higher alpha smooth muscle actin levels indicated a higher number of myoepithelial cells in the p53^{+/+} tumors, we performed immunohistochemistry with alpha

smooth muscle actin antibodies on fixed sections of p53^{+/+} and p53^{-/-} tumors. As shown in Figure 4, the staining patterns in the p53^{+/+} tumors reveal staining around the more organized glandular structures, consistent with a myoepithelial cell localization. In contrast, the staining for alpha smooth muscle actin in the p53^{-/-} tumors is not only reduced in intensity and frequency, but appears in a more random disorganized pattern associated with the tumor stroma. These results are consistent with a more differentiated structural organization in the p53^{+/+} tumors than in their p53^{-/-} counterparts.

Discussion

We believe that the *Wnt-1* TG/p53 model provides a number of advantages for mechanistic studies on the role of p53 in tumorigenesis. Virtually all of the *Wnt-1* TG females develop only mammary adenocarcinomas within 2–9 months either in the presence or absence of p53. In this model, the absence of p53 has been shown to dramatically alter the biological and genetic properties of the *Wnt-1*-initiated adenocarcinomas. An important question is whether the more aggressive and malignant characteristics of the p53^{-/-} tumors are a direct result of the absence of p53 or an indirect result of the genomic instability promoted by the lack

of p53. In this latter scenario, the driving force for tumor initiation and progression would be the increased rate of cooperating genetic lesions in the p53^{-/-} tumors. However, if p53 were playing a more active role in inhibition of tumor growth through its transcriptional regulatory function, then upregulation of p53 growth inhibitory targets and downregulation of p53 growth stimulatory targets might be observed. In fact, the increase in p21 and cyclin G1 levels and decreased cyclin B1 levels observed in the p53^{+/+} tumors are consistent with a direct role for p53 in modulating tumor growth rates. Moreover, the upregulation of several differentiation markers in the p53^{+/+} tumors, some direct targets of p53, suggests that these genes may be contributing to some of the biological properties of the tumors. Finally, the increased activities of the known p53 target genes in the p53^{+/+} tumors indicates that p53 signaling pathways are intact in these tumors, and that tumors can readily arise in this model in the presence of functional p53.

The differentially expressed genes that have been identified in this model fall generally into two categories, growth regulatory genes (p21, cyclin G1, cyclin B1, and *c-kit*) and differentiation markers (alpha smooth muscle actin, kappa casein, and cytokeratin 19). Some of the other categories of p53 target genes found in cell based screens, such as apoptosis-related

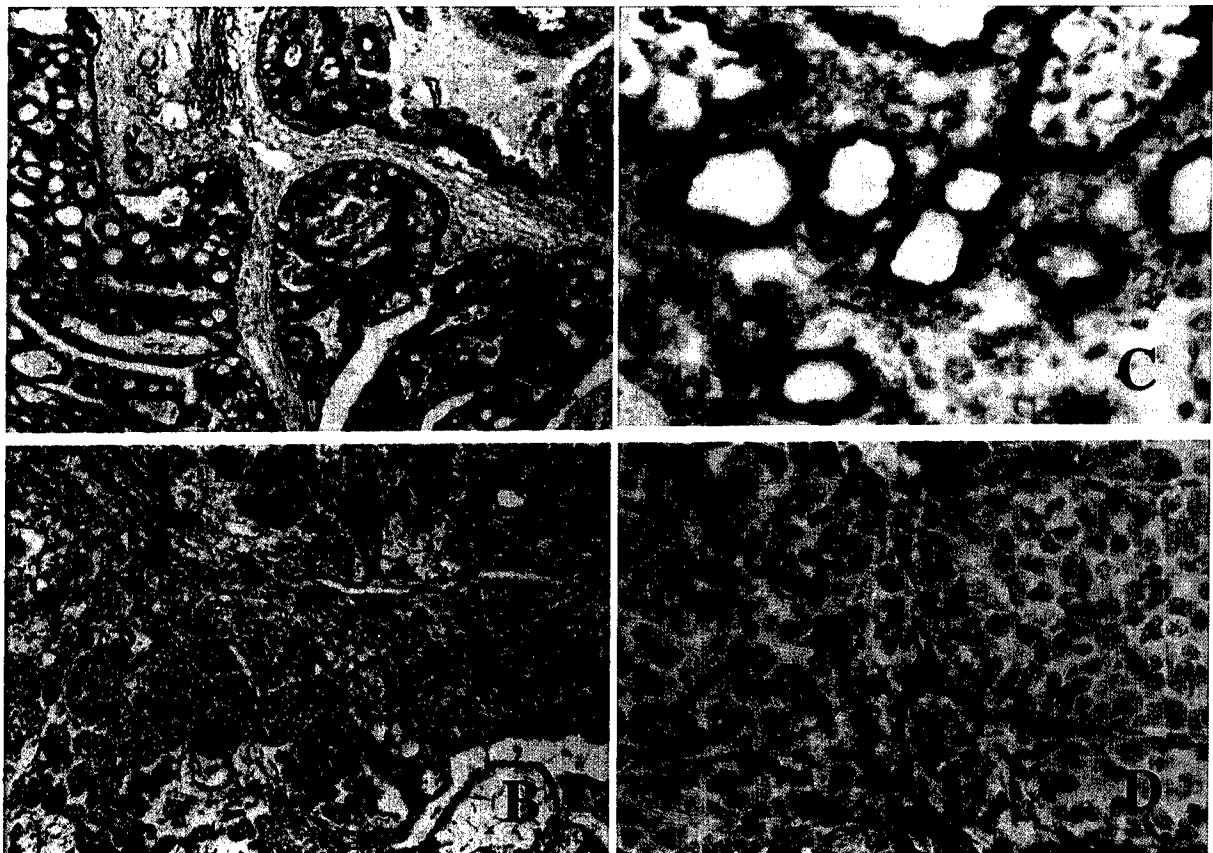


Figure 4 Immunohistochemistry on fixed *Wnt-1* TG p53^{+/+} and *Wnt-1* TG p53^{-/-} mammary tumor sections with alpha smooth muscle actin antibodies. Panels (a) and (c) show a representative *Wnt-1* TG p53^{+/+} mammary tumor at 100 \times and 400 \times magnification, respectively. Panels (b) and (d) show a representative *Wnt-1* TG p53^{-/-} mammary tumor at 100 \times and 400 \times magnification, respectively. The intense brown staining in the glandular structures of the p53^{+/+} tumors and comparatively low levels of staining in the more disorganized structures of the p53^{-/-} tumors is consistent with the increased levels of alpha smooth muscle RNA and protein in the p53^{+/+} tumors as assayed by the Northern and Western blot analyses

genes and genes which regulate reactive oxygen species formation, have not been identified as differentially expressed genes in any of our tumor screens. This finding agrees with earlier findings by Yu *et al.* (1999) that the responses by p53 targets can vary considerably from cell line to cell line. Moreover, because in our model p53 is expressed at physiological levels in an *in vivo* heterogeneous context of mixed cell types, it is not surprising that the range of p53 targets observed is quite different from the cell based screens. However, the specific nature of the genes that are differentially expressed in our model is consistent with their playing a direct role in modulating the biological properties of the tumors. The potential relevance of each differentially expressed gene to the tumorigenesis process is discussed below.

Differentially expressed growth regulatory genes

p21^{WAF1/CIP1} p21^{WAF1/CIP1} is a prototypical p53 target gene activated by p53 in response to a variety of cell stresses (Gorospe *et al.*, 1999). It is a cyclin-dependent kinase inhibitor which has both G1 and G2 checkpoint functions in response to DNA damage (Harper *et al.*, 1995; Dulic *et al.*, 1998; Bunz *et al.*, 1998). Its higher levels of expression in the presence of p53 may directly reduce tumor growth rates as observed in previous studies on the *Wnt-1* TG model. In these studies we found that *Wnt-1* TG p21^{+/-} mammary tumors had dramatically higher growth rates compared to *Wnt-1* TG p21^{+/+} tumors (Jones *et al.*, 1999). In addition, maintenance of G1 and G2 checkpoints in the p53^{+/+} tumors (in part through increased p21) may also contribute to the relatively high levels of genomic stability observed in this category of tumors.

Cyclin B1 Cyclin B1 is the major cyclin component of the mitotic cdc2-cyclin B complex initiating mitosis in eukaryotic cells (Musunuru and Hinds, 1997). It is upregulated in expression in the G2/M phase of the cell cycle. Recently, it has been demonstrated that p53 directly represses transcription of the cyclin B1 gene and thus may affect G2/M transition by reducing intracellular cyclin B1 levels (Innocente *et al.*, 1999; Taylor *et al.*, 1999). p21 has also been shown to inhibit the kinase activity of the cyclin B1-cdc2 complex (Xiong *et al.*, 1993; Harper *et al.*, 1995) and so p53 may mediate the G2 checkpoint through multiple mechanisms. Such mechanisms may contribute to the reduced rate of cell cycle progression and increased genomic stability observed in the p53^{+/+} tumors (Donehower *et al.*, 1995; Jones *et al.*, 1997).

Cyclin G1 Cyclin G1 has been shown to be transcriptionally activated by p53 in response to DNA damage (Okamoto and Beach, 1994). The role of cyclin G1 in cell cycle control has not been established and published reports are contradictory as to whether cyclin G1 is growth promoting or growth inhibitory (Smith *et al.*, 1997; Shimizu *et al.*, 1998). Recently, however, it has been shown that over-expression of cyclin G augments the apoptosis process (Okamoto and Prives, 1999). However, since apoptosis levels are low in the p53^{+/+} tumors, it is not clear how increased cyclin G1 levels in these tumors might affect their biological properties.

c-kit *c-kit* encodes a membrane tyrosine kinase receptor and is not known to be a direct target of p53. Its ligand is stem cell factor, which promotes growth in a number of hematopoietic precursor types (Ashman, 1999). Mutated versions of kit can be oncogenic and it is expressed at high levels in small cell lung carcinomas (Hibi *et al.*, 1991). However, in other types of human cancers, such as melanomas, thyroid carcinomas, and breast cancers, *c-kit* expression was reduced as the tumors progressed from normal tissues to benign lesions to malignant cancers (Natali *et al.*, 1992a,b, 1995). Moreover, ectopic expression of *c-kit* in breast cancer cells suppressed their growth (Nishida *et al.*, 1996), indicating that in mammary cells, *c-kit* may act as a tumor suppressor. Thus, in our mammary cancer model, the increased expression of *c-kit* in the p53^{+/+} tumors may not only be a marker for a less malignant status, but may also be directly active in suppressing tumor cell growth rates.

Differentially expressed differentiation markers

Alpha smooth muscle actin Alpha smooth muscle actin is a major component of microfilaments and assists in maintaining cell shape and movement. It has been shown to be a p53 target gene (Comer *et al.*, 1998) and is also a marker for the myoepithelial cell compartment of the mammary gland (Gugliotta *et al.*, 1988). Alpha smooth muscle actin is downregulated in transformed cells and an inverse relationship between cellular proliferation and alpha smooth muscle actin expression has been widely observed (Leavitt *et al.*, 1985; Owens *et al.*, 1986). In the p53^{+/+} tumors, it appears to be highly expressed in myoepithelial cells, a compartment which is present in lower quantities in the p53^{-/-} tumors (Figure 4). Thus, higher expression levels of this p53 responsive gene is a good indicator of retention of more differentiated cell types in the p53^{+/+} tumors. Whether alpha smooth muscle actin has a role in the inhibition of tumor growth rates is unclear.

Cytokeratin 19 Cytokeratin 19 is one of the constituents of the intermediate filaments of epithelial cells and has recently been shown to be a p53 target gene (Zhao *et al.*, 2000). Cytokeratin 19 is a widely used luminal cell epithelial marker which is expressed at high levels in both normal and malignant human mammary epithelial cells (Moll and Schramm, 1998). It is expressed at high levels in many of the p53^{+/+} tumors, indicating the presence of significant numbers of luminal epithelial cells in the tumors. However, the p53^{-/-} tumors display lower levels of cytokeratin 19 mRNA and protein, indicating that either these tumors have lost most of their luminal epithelial cells or that the luminal epithelial cells in these tumors have somehow lost cytokeratin 19 expression.

Kappa casein Kappa casein is not considered to be a p53 target, but is a milk protein specific for secretory alveolar cells in the mammary gland (Ginger and Grigor, 1999). It is found at high levels in normal breast tissue, lower levels in benign lesions, and not at all in invasive carcinomas (Rudland *et al.*, 1993). Its increased levels in the p53^{+/+} tumors are consistent with the relatively differentiated state of these tumors. It also indicates retention of some functional secretory

alveolar cells in the p53^{+/+} tumors and their loss in the more dedifferentiated p53^{-/-} tumors.

Conclusions

The identification of differentially expressed growth-related genes in our model is consistent with the observed differences in tumor growth rates between the p53^{+/+} and p53^{-/-} mice. Interestingly, three of four of these genes are p53 target genes, indicating that wild type p53 is actively regulating expression of these genes. We hypothesize that such p53 signaling inhibits cell cycle progression in the p53^{+/+} tumor cells and may be at least partially responsible for their slower growth rate. The retention of G1 and G2 checkpoint control in the p53^{+/+} tumors may also contribute to the slower growth rate and delayed tumor incidence by preventing genomic instability and the resultant increase in oncogenic mutations.

The higher expression of differentiation markers in the p53^{+/+} tumors, such as alpha smooth muscle actin and kappa casein, is consistent with their more differentiated histopathological appearance. Since these two genes have been associated with myoepithelial and secretory alveolar cell types, respectively, it is likely that such differentiated cell types are lost in the progression of the p53^{-/-} tumors to a more dedifferentiated state. In human breast neoplasms, benign lesions show retention of myoepithelial and secretory alveolar cells, while in invasive carcinomas they are almost completely lost (Rudland *et al.*, 1993). Thus, the p53^{+/+} tumors are likely to represent a more benign stage of mammary tumor progression, while the p53^{-/-} tumors may be models for the more invasive stages of mammary carcinomas.

Another interpretation of the p53^{+/+} and p53^{-/-} tumor differences is that they are derived from fundamentally different cells of origin. Wynford-Thomas has noted that about one-third of human invasive ductal breast cancers fall into a more aggressive subgroup which can be defined by poor differentiation, high proliferative rate, and estrogen receptor negativity (Wynford-Thomas, 1997). It was suggested that this subgroup may have arisen from a less-differentiated breast epithelial type such as a mammary stem cell. Interestingly, this aggressive subgroup of breast cancers has also been shown to correlate with a very high rate of p53 mutation (Thor *et al.*, 1992; Mazars *et al.*, 1992). The predominant, well-differentiated 'luminal' tumor type in humans and the *Wnt-1* TG p53^{+/+} model may retain wild type p53 because there is little selective advantage for p53 mutation, whereas mutation of p53 in the mammary stem cells may provide a more profound advantage. This model is consistent with the idea that the *Wnt-1* TG p53^{-/-} tumors arise from an undifferentiated mammary stem cell while the *Wnt-1* TG p53^{+/+} tumors arise from a more differentiated mammary cell type.

Despite the limitations inherent in doing expression analyses on end stage heterogeneous tumors, differentially expressed genes were identified in multiple p53^{+/+} and p53^{-/-} tumors. The differentially expressed genes that were obtained were either growth regulators or indicators of cell differentiation status and were consistent with the differential histopathology

and biological properties of the p53^{+/+} and p53^{-/-} tumors. Moreover, these results and the fact that many of these genes were *bona fide* direct transcriptional targets of p53 lends support to our argument that screening of whole tumors is a viable approach for identifying such genes. Further screens with large cDNA arrays should reveal additional differentially expressed genes. A remaining challenge will be to determine which of these differentially expressed genes have a direct effect on the biological properties of the mammary adenocarcinomas.

Materials and methods

Tumor samples

The *Wnt-1* TG/p53 mammary cancer model from which the mammary tumors have been obtained has been previously described (Donehower *et al.*, 1995). *Wnt-1* TG p53^{+/+}, *Wnt-1* TG p53^{+/-}, and *Wnt-1* TG p53^{-/-} females were monitored for tumors on a weekly basis from the time of weaning until the first observation of tumors. Four weeks after first observation of a tumor, the tumor bearing animal was sacrificed and the tumor excised. The skin and connective tissue were removed carefully and part of the tumor was placed in 10% neutral buffered formalin and the remainder was frozen in an Eppendorf tube at -80°C. The tumor segment in formalin was then fixed in paraffin and hematoxylin and eosin stained slides made from 4 μ sections of tumor tissue. These sections were then typed by histopathological examination and virtually all were categorized as Dunn type B mammary adenocarcinomas. In preparation for the various RNA assays described below, mRNA was purified from frozen tumor segments utilizing the Invitrogen mRNA extraction kit according to the manufacturer's specifications.

Differential display

The Clontech Delta Differential Display kit was used to screen tumor RNAs derived from p53^{+/+} and p53^{-/-} mammary tumors. RNAs from p53^{+/-} tumors that had lost their remaining wild type p53 allele (p53^{+/-} LOH) were also utilized. These tumors were similar in their histopathological and biologic properties to p53^{-/-} tumors. The protocols were all performed according to the manufacturer's instructions and will only be outlined here. Initially, the first strand cDNA is synthesized from each of the tumor RNA populations of interest, using murine leukemia virus reverse transcriptase and oligo(dT) as a primer. For differential display PCR, 10 arbitrary 5' primers (oligo(dT)₉-NN, where N=A,G, or C) were combined with 10 arbitrary 3' primers randomly in a PCR reaction in the presence of alpha-³²P-dATP. To resolve the PCR-amplified labeled cDNA fragments, a denaturing 5% polyacrylamide/8 M urea gel was used. After electrophoresis, the denaturing gels were subjected to autoradiography and the X-ray films were carefully examined for differentially expressed bands. Generally, multiple tumor RNAs of each genotype were run in parallel to identify fragments which were consistently overexpressed or underexpressed in a particular genotype. Once differentially expressed bands were identified, they were excised from the gel, placed in TE buffer (10 mM Tris-HCl, pH 8.0, 1 mM EDTA), and the cDNA fragments were eluted from the gel slice by boiling. The DNA was then reamplified using the original 5' and 3' arbitrary primers. ³²P-labeled probes were made from the reamplified fragments by the random primed oligo labeling procedure using the Roche High Prime kit and used to probe Northern blots of RNAs from 6-8 p53^{+/+} and 6-8 p53^{-/-} tumors. Those probes

that showed consistent p53 genotype-specific overexpression or underexpression were ligated into a Clontech TA cloning vector using the Clontech AdvanTAGE PCR cloning kit according to the manufacturer's specifications. Positive clones were amplified and sequenced with the M13 forward primer and the Amersham Sequenase kit. About 200–300 base pairs of insert sequences were identified by this method and these were used to probe GenBank in homology searches.

Northern blot hybridization

For Northern blot analysis, the Ambion NorthernMax kit was used according to manufacturer directions. Two μg of mRNA from 5–8 p53+/+ tumors and 5–8 p53-/- tumors were loaded in each well of the agarose gel. After electrophoresis, the separated RNAs were transferred to a Zeta-Probe membrane from Bio-Rad. Labeled ^{32}P probes for each differentially expressed gene were hybridized to the membranes. After hybridization, membrane washing, and autoradiography, the band hybridization intensities on the filters were quantitated on the Molecular Dynamics Storm 860 Phosphorimager. The filters were then stripped and reprobed with a labeled GAPDH probe to provide a normalization control. After autoradiography, this filter was also subjected to phosphorimager analysis. Relative hybridization intensities for a particular gene in a tumor were always normalized to the intensity of the GAPDH signal in that tumor to obtain quantitative values.

cDNA arrays

The Clontech Atlas mouse array I with 588 known cDNAs attached to duplicate nylon membranes was used for the cDNA array screen. One μg of mRNA from a p53-/- tumor and a p53+/+ tumor were each reverse transcribed in the presence of alpha ^{32}P -dATP. The labeled cDNA populations were then each hybridized overnight to the two array filters according to the manufacturer's specifications. After washing and autoradiography, the hybridization intensity of each of the genes on the filter was quantitated by phosphorimager analysis. Spot intensities were then normalized to the intensities of housekeeping genes on the filter to estimate relative hybridization levels between the p53+/+ and p53-/- filters. Genes that repeatedly showed more than 2.5-fold differences in hybridization intensity between the two filters were assessed for differential expression by Northern blot hybridization after synthesis of probes by RT-PCR using gene specific primers.

RNAse protection assay

RNA expression levels of 14 cyclin genes in the p53+/+ and p53-/- tumors were assessed using two Pharmingen multi-probe RNAse protection assay kits (mcy-1 and mcy-2). ^{32}P -labeled RNA mouse cyclin probes were generated by T7 RNA polymerase-directed synthesis of 14 different cyclin gene templates. The multi-probe set was then hybridized in excess to target RNA (10 μg mRNA for each sample) in solution, after which free probes and other single-stranded RNA are digested with RNAses. The remaining RNAse protected probes were purified, resolved on denaturing polyacrylamide gels, and quantified by phosphorimaging. The quantity of each mRNA species in the original RNA sample could then be determined based on the intensity of the appropriately sized protected probe fragment following normalization to a control probe (GAPDH) used along with the cyclin probes.

Immunoblot assays

Western blot analysis of alpha smooth muscle actin, cytokeratin 19, *c-kit*, cyclin B1 and cyclin G1 protein was performed from tumor lysates of multiple p53+/+ and p53-/- tumors. For alpha smooth muscle actin protein detection, 20 μg of total tumor lysate was run on an 8% SDS polyacrylamide gel. The gel was transferred to a 0.45 μm pore size nitrocellulose membrane (BA85, Schleicher & Schuell) for 2 h at 75 volts and then blocked with 5% nonfat dry milk in Tris-buffered saline with 2% Tween 20 (TBST) overnight at 4°C. The blot was incubated with mouse monoclonal antibody for alpha smooth muscle actin (Clone 1A4 from NeoMarkers) diluted at 1:1000 in TBST with 1% nonfat dry milk for 1 h at room temperature. After washing three times with TBST, the blot was incubated with goat anti-mouse IgG2a peroxidase. Protein was detected using the supersignal enhanced chemiluminescence (ECL) system (Pierce). For cytokeratin 19 detection, 50 μg protein lysate was loaded for gel separation. The antibody used for cytokeratin 19 was Clone A53-B from NeoMarkers. Dilution and incubation conditions were the same as for alpha-smooth muscle actin. *c-kit* antibody (M-14, Santa Cruz) was diluted 1:200. Antigoat IgG was diluted 1:2000 as secondary antibody. For cyclin B1 detection, 20 μg protein lysate was loaded on an SDS-polyacrylamide gel. After transfer to a nitrocellulose membrane, the blot was incubated with a polyclonal antibody to cyclin B1 (Oncogene Research Ab-3) diluted 1:2000. For cyclin G1 analysis, 100 μg of tumor lysate was loaded on a 12% SDS-polyacrylamide gel. Cyclin G1 antibody (C-18, Santa Cruz) was diluted 1:200 for the Western blot. Goat anti-rabbit antibody (SC-2030, Santa Cruz) was diluted 1:1000 as secondary antibody. Each blot was stripped and reprobed with an antibody against all six isoforms of vertebrate actin (C4, Boehringer-Mannheim) as a loading control.

Immunohistochemistry on tumor sections

Tumor samples were fixed with neutral buffered formalin and embedded in paraffin. Tumor slides were deparaffinized, rehydrated, and treated with 3% H_2O_2 to quench any endogenous peroxidase. Samples were then boiled in 10 mM sodium citrate buffer (pH 6) for 10 min to unmask the antigen. After washing with PBS, the slides were blocked with 10% goat serum at room temperature for 30 min and then incubated with 1:200 mouse monoclonal antibody (1A4, NeoMarkers) at 4°C overnight. After warming up to room temperature, the slides were washed with PBS and incubated with 1:400 peroxidase-coupled secondary antibody (goat anti-mouse, Boehringer-Mannheim) for 1 h. The antibody-antigen reaction was visualized by DAB staining and counterstained with hematoxylin.

Acknowledgments

We would like to thank Harold Varmus for providing us with the *Wnt-1* TG mice. We also thank Dan Medina for helpful discussions and for histopathological analyses of the tumors. This work was supported by grants from the National Cancer Institute and the US Army Breast Cancer Program to L Donehower. L Donehower is the recipient of an Academic Award from the US Army Breast Cancer Program. X-S Cui was supported by the Karolinska Institute/Baylor College of Medicine Exchange Program and the US Army Breast Cancer Research Program.

References

- Ashman LK. (1999). *Int. J. Biochem. Cell Biol.*, **31**, 1037–1051.
- Bunz F, Dutriaux A, Lengauer C, Waldman T, Zhou S, Brown JP, Sedivy JM, Kinzler KW and Vogelstein B. (1998). *Science*, **282**, 1497–1501.
- Comer KA, Dennis PA, Armstrong L, Catino JJ, Kastan MB and Kumar CC. (1998). *Oncogene*, **16**, 1299–1308.
- Donehower LA. (1996). *Biochim. Biophys. Acta*, **1242**, 171–176.
- Donehower LA, Godley LA, Aldaz CM, Pyle R, Shi YP, Pinkel D, Gray J, Bradley A, Medina D and Varmus HE. (1995). *Genes Dev.*, **9**, 882–895.
- Dulic V, Stein GH, Far DF and Reed SI. (1998). *Mol. Cell Biol.*, **18**, 1546–1557.
- el-Deiry WS. (1998). *Semin. Cancer Biol.*, **8**, 345–357.
- el-Deiry WS, Tokino T, Velculesco VE, Levy DB, Parsons R, Trent JM, Lin D, Mercer WE, Kinzler KW and Vogelstein B. (1993). *Cell*, **75**, 817–825.
- Freedman DA, Wu L and Levine AJ. *Cell. Mol. Life Sci.*, **55**, 96–107.
- Giaccia AJ and Kastan MB. (1998). *Genes Dev.*, **12**, 2973–2983.
- Ginger MR and Grigor MR. (1999). *Comp. Biochem. Physiol. B. Biochem. Mol. Biol.*, **124**, 133–145.
- Gorospe M, Wang X and Holbrook NJ. (1999). *Gene Exp.*, **7**, 377–385.
- Gugliotta P, Sapino A, Macri L, Skalli O, Gabbiani G and Bussolati G. (1988). *J. Histochem. Cytochem.*, **36**, 659–663.
- Harper JW, Adami GR, Wei N, Keyomarsi K and Elledge SJ. (1993). *Cell*, **75**, 805–816.
- Harper JW, Elledge SJ, Keyomarsi K, Dynlacht B, Tsai LH, Zhang P, Dobrowolski S, Bai C, Connell-Crowley L, Swindell E, Fox MP and Wei N. (1995). *Mol. Biol. Cell.*, **6**, 387–400.
- Hibi K, Takahashi T, Sekido Y, Ueda R, Hida T, Ariyoshi Y, Takagi H and Takahashi T. (1991). *Oncogene*, **6**, 2291–2296.
- Innocente SA, Abrahamson JL, Cogswell JP and Lee JM. (1999). *Proc. Natl. Acad. Sci. USA*, **96**, 2147–2152.
- Jones JM, Attardi L, Godley LA, Laucirica R, Medina D, Jacks T, Varmus HE and Donehower LA. (1997). *Cell Growth Diff.*, **8**, 829–838.
- Jones JM, Cui XS, Medina D and Donehower LA. (1999). *Cell Growth Diff.*, **10**, 213–222.
- Kirsch DG and Kastan MB. (1998). *J. Clin. Oncol.*, **16**, 3158–3168.
- Leavitt J, Gunning P, Kedes L and Jariwalla R. (1985). *Nature*, **316**, 840–842.
- Levine AJ. (1997). *Cell*, **88**, 323–331.
- Liang P and Pardee AB. (1992). *Science*, **257**, 967–971.
- Lozano G and Elledge SJ. (2000). *Nature*, **404**, 24–25.
- Mazars R, Spinardi L, BenCheikh M, Simony-Lafontaine J, Jeanteur P and Theillet C. (1992). *Cancer Res.*, **52**, 3918–3923.
- Miyashita T and Reed JC. (1995). *Cell*, **80**, 293–299.
- Moll UM and Schramm LM. (1998). *Crit. Rev. Oral Biol. Med.*, **9**, 23–37.
- Musunuru K and Hinds PW. (1997). *Cell Cycle Regulators in Cancer*. Karger Landes Systems, Basel.
- Natali PG, Nicotra MR, Winkler AB, Cavaliere R, Bigotti A and Ullrich A. (1992a). *Int. J. Cancer*, **52**, 197–201.
- Natali PG, Nicotra MR, Sures I, Mottolese M, Botti C and Ullrich A. (1992b). *Int. J. Cancer*, **52**, 713–717.
- Natali PG, Berlingieri MT, Nicotra MR, Fusco A, Santoro E, Bigotti A and Vecchio G. (1995). *Cancer Res.*, **55**, 1787–1791.
- Nishida K, Tsukamoto T, Uchida K, Takahashi T, Takahashi T and Ueda R. (1996). *Anticancer Res.*, **16**, 3397–3402.
- Okamoto K and Beach D. (1994). *EMBO J.*, **13**, 4816–4822.
- Okamoto K and Prives C. (1999). *Oncogene*, **18**, 4606–4615.
- Owens GK, Loeb A, Gordon D and Thompson MM. (1986). *J. Cell Biol.*, **102**, 343–352.
- Rudland PS, Leinster SJ, Winstanley J, Green B, Atkinson M and Zakhour HD. (1993). *J. Histochem. Cytochem.*, **41**, 543–553.
- Polyak K, Xia Y, Zweier JL, Kinzler KW and Vogelstein B. (1997). *Nature*, **389**, 300–305.
- Shimizu A, Nishida J, Ueoka Y, Kato K, Hachiya T, Kuriaki Y and Wake N. (1998). *Biochem. Biophys. Res. Commun.*, **242**, 529–533.
- Smith ML, Kontny HU, Bortnick R and Fornace Jr AJ. (1997). *Exp. Cell Res.*, **230**, 61–68.
- Taylor WR, DePrimo SE, Agarwal A, Agarwal ML, Schonthal AH, Katula KS and Stark GR. (1999). *Mol. Biol. Cell.*, **10**, 3607–3622.
- Thor AD, Moore II DH, Edgerton SM, Kawasaki ES, Reihnsaus E, Lynch HT, Marcus JN, Schwartz L, Chen LC, Mayall BH and Smith HS. (1992). *J. Natl. Cancer Inst.*, **84**, 845–855.
- Tsukamoto AS, Grosschedl R, Guzman RC, Parslow T and Varmus HE. (1988). *Cell*, **55**, 619–625.
- Wallace-Brodeur RR and Lowe SW. (1999). *Cell. Mol. Life Sci.*, **55**, 64–75.
- Wynford-Thomas D. (1997). *Eur. J. Cancer*, **33**, 716–726.
- Xiong Y, Hannon GJ, Zhang H, Casso D, Kobayashi R and Beach D. (1993). *Nature*, **366**, 701–704.
- Yu J, Zhang L, Hwang PM, Rago C, Kinzler KW and Vogelstein B. (1999). *Proc. Natl. Acad. Sci. USA*, **96**, 14517–14522.
- Zhao R, Gish K, Murphy M, Yin Y, Notterman D, Hoffman WH, Tom E, Mack DH and Levine AJ. (2000). *Genes Dev.*, **14**, 981–993.

Cell cycle-regulated phosphorylation of p220^{NPAT} by cyclin E/Cdk2 in Cajal bodies promotes histone gene transcription

Tianlin Ma,¹ Brian A. Van Tine,^{4,5} Yue Wei,² Michelle D. Garrett,⁶ David Nelson,⁷
Peter D. Adams,⁷ Jin Wang,^{1,3} Jun Qin,^{1,3} Louise T. Chow,⁴ and J. Wade Harper^{1,2}

¹Department of Biochemistry and Molecular Biology, ²Department of Molecular Physiology and Biophysics, ³Department of Molecular and Cellular Biology, Baylor College of Medicine, Houston, Texas 77030, USA; ⁴Department of Biochemistry and Molecular Genetics, ⁵Department of Pathology, University of Alabama, Birmingham, Alabama 35294, USA; ⁶CRC Centre for Cancer Therapeutics, Institute of Cancer Research, Sutton, SM2 5NG, United Kingdom; ⁷Fox Chase Cancer Center, Philadelphia, Pennsylvania 19111, USA

Cell cycle-regulated phosphorylation of p220^{NPAT} by cyclin E/Cdk2 in Cajal bodies promotes histone gene transcription

Tianlin Ma,^{1,8} Brian A. Van Tine,^{4,5,8} Yue Wei,² Michelle D. Garrett,⁶ David Nelson,⁷ Peter D. Adams,⁷ Jin Wang,^{1,3} Jun Qin,^{1,3} Louise T. Chow,⁴ and J. Wade Harper^{1,2,9}

¹Department of Biochemistry and Molecular Biology, ²Department of Molecular Physiology and Biophysics, ³Department of Molecular and Cellular Biology, Baylor College of Medicine, Houston, Texas 77030, USA; ⁴Department of Biochemistry and Molecular Genetics, ⁵Department of Pathology, University of Alabama, Birmingham, Alabama 35294, USA; ⁶CRC Centre for Cancer Therapeutics, Institute of Cancer Research, Sutton, SM2 5NG, United Kingdom; ⁷Fox Chase Cancer Center, Philadelphia, Pennsylvania 19111, USA

Cyclin E/Cdk2 acts at the G1/S-phase transition to promote the E2F transcriptional program and the initiation of DNA synthesis. To explore further how cyclin E/Cdk2 controls S-phase events, we examined the subcellular localization of the cyclin E/Cdk2 interacting protein p220^{NPAT} and its regulation by phosphorylation. p220 is localized to discrete nuclear foci. Diploid fibroblasts in G₀ and G₁ contain two p220 foci, whereas S- and G₂-phase cells contain primarily four p220 foci. Cells in metaphase and telophase have no detectable focus. p220 foci contain cyclin E and are coincident with Cajal bodies (CBs), subnuclear organelles that associate with histone gene clusters on chromosomes 1 and 6. Interestingly, p220 foci associate with chromosome 6 throughout the cell cycle and with chromosome 1 during S phase. Five cyclin E/Cdk2 phosphorylation sites in p220 were identified. Phospho-specific antibodies against two of these sites react with p220 within CBs in a cell cycle-specific manner. The timing of p220 phosphorylation correlates with the appearance of cyclin E in CBs at the G₁/S boundary, and this phosphorylation is maintained until prophase. Expression of p220 activates transcription of the histone H2B promoter. Importantly, mutation of Cdk2 phosphorylation sites to alanine abrogates the ability of p220 to activate the histone H2B promoter. Collectively, these results strongly suggest that p220^{NPAT} links cyclical cyclin E/Cdk2 kinase activity to replication-dependent histone gene transcription.

[Key Words: Cyclin-dependent kinases; phosphorylation; Cajal (coiled) bodies; histone transcription]

Received June 23, 2000; revised version accepted August 1, 2000.

Cyclin E, an essential regulatory subunit of Cdk2 (Dulic et al. 1992; Koff et al. 1992), plays a central role in coordinating both the onset of S phase and centrosome duplication in multicellular eukaryotes (Sherr 1996; Reed 1997). Cyclin E/Cdk2 complexes have two major roles in promoting S phase. First, cyclin E/Cdk2 participates, together with cyclin D/Cdk4, in the control of transcriptional processes that are critical to cell cycle progression. The best understood example is control of the E2F/DP transcription factor via phosphorylation of a family of transcriptional repressors (Rb, p130, and p107) (for review, see Reed 1997; Dyson 1998; Nevins 1998). E2F complexes regulate the S-phase-dependent expression of a number of proteins required for the synthesis of nucleic acids as well as proteins such as Cdc2 and cyclin A that promote subsequent cell cycle transitions. Second, cyc-

lin E/Cdk2 can function in an E2F-independent manner to activate DNA replication. Accumulation of cyclin E is required for S-phase entry, and ectopic cyclin E expression can bypass the requirement for Rb inactivation and E2F activation for S-phase entry (Ohtsubo et al. 1995; Leng et al. 1997; Lukas et al. 1997).

An understanding of the role of cyclin E/Cdk2 in promoting S phase requires knowledge of its essential substrates. Insight into Cdk targets has been advanced by the finding that several Cdk substrates bind tightly to the cyclin subunit. In some cases, this interaction involves a motif in the substrate, the RXL motif, and a conserved pocket in the cyclin box (Zhu et al. 1995; Adams et al. 1996; Russo et al. 1996; Schulman et al. 1998; Brown et al. 1999; Ma et al. 1999). We and others have exploited this property of cyclins to identify relevant cyclin E/Cdk2 substrates with the use of expression cloning (Zhao et al. 1998; Ma et al. 1999). One of these, p220^{NPAT}, interacts with cyclin E/Cdk2 in extracts from tissue culture cells and accelerates S-phase entry when overexpressed (Zhao et al. 1998). Moreover, retroviral insertion into the mouse p220^{NPAT} gene leads to embry-

⁸These authors contributed equally to this work.

⁹Corresponding author.

E-MAIL jharper@bcm.tmc.edu; FAX (713) 796-9438.

Article and publication arc at www.genesdev.org/cgi/doi/10.1101/gad.829500.

onic lethality at the eight-cell stage, indicating an essential role for p220 in cell division or development (Di Fruscio et al. 1997). However, the precise function of p220 and the role of cyclin E/Cdk2 in its action remain unknown.

Emerging data (Zhao et al. 2000, this paper) suggest that p220 is involved in S-phase-specific histone gene transcription. Histones, components of nucleosomes, have to be supplied on demand during DNA replication. This regulation is attributed to both transcriptional and posttranscriptional control mechanisms (Harris et al. 1991; Heintz 1991), mediated in part by the activation of histone gene-specific transcription factors (Oct-1 in the case of the H2B promoter and H1TF2 in the case of the H1 promoter) through an unknown mechanism (Fletcher et al. 1987; Segil et al. 1991). Once generated, histone messages are stabilized and processed preferentially in S phase. Implicated in histone gene transcription are Cajal bodies (CBs; sometimes referred to as coiled bodies). CBs were initially described as small nuclear organelles (Cajal 1903), but their function has remained obscure for the better part of the twentieth century. Recent work has led to the hypothesis that CBs are sites of assembly of transcription and splicing complexes (Gall et al. 1999). The link to histone transcription comes from the finding that a subset of CBs is physically associated with histone gene clusters on chromosomes 1 (1q21) and 6 (6p21) (Frey and Matera 1995) and with histone gene loci in *Xenopus* lampbrush chromosomes (Abbott et al. 1999). Moreover, CBs also contain a component of the histone mRNA 3'-end processing machinery SLBP1 (Abbott et al. 1999).

Here, we report that p220^{NPAT} is localized to discrete foci that are coincident with a subset of CBs in normal diploid fibroblasts. The number of p220 foci increased from two in G₀ and G₁ cells in association with chromosome 6 to four in S and G₂ phases in association with both chromosomes 6 and 1. Foci are lost during mitosis. Consistent with these observations, Zhao et al. (2000) have found that p220 is associated directly with histone gene clusters and that overexpression of p220 can activate histone 2B and histone 4 transcription. We also demonstrate that cyclin E is contained in p220 foci and that p220 within CBs is phosphorylated on Cdk sites in a cell cycle-dependent manner. Moreover, mutation of cyclin E/Cdk2 phosphorylation sites in p220 reduces its ability to activate expression from histone H2B reporter constructs in transiently transfected cells. These data, together with those of Zhao et al. (2000), suggest that cyclin E/Cdk2 functions in conjunction with p220 to coordinate S-phase-dependent histone gene transcription; they also demonstrate a role for CBs in cell cycle-regulated transcriptional control.

Results

p220 is localized in cell cycle-regulated nuclear foci

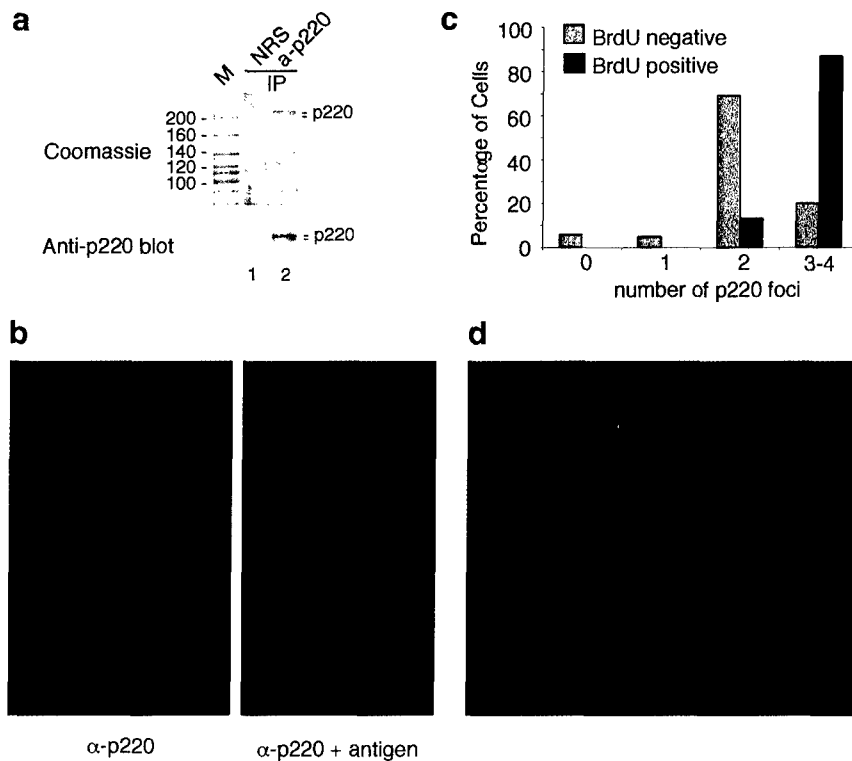
We previously identified a C-terminal fragment of NPAT (residues 1054–1397) in a cyclin E/Cdk3 interaction screen (Ma et al. 1999). Affinity-purified anti-NPAT an-

tibodies generated against this C-terminal fragment recognize a closely spaced protein doublet of 220 kD in molecular mass in nuclear extracts from HeLa and 293 cells, as determined by either immunoblotting or immunoprecipitation (Fig. 1a, lane 2; data not shown). The identity of the p220 protein obtained by immunoprecipitation was confirmed by mass spectral analysis of tryptic peptides (see below).

To examine the subcellular localization of p220, we performed immunofluorescence by using normal diploid fibroblasts (Fig. 1b). The majority of cells (>80%) in an asynchronous culture contained either two or four nuclear foci staining for p220, whereas the remaining cells contained one or three obvious p220 foci. This immunoreactivity was blocked by competition with antigen (Fig. 1b). The variation of p220 staining patterns suggested that p220 localization might be cell cycle regulated. To test this possibility, we examined p220 localization in several asynchronous growing fibroblast lines (normal dermal fibroblasts, WI38 fibroblasts, and bjTERT fibroblasts) labeled with BrdU to mark S-phase cells. Similar results were observed, and the data for bjTERT cells are shown in Figure 1c,d. The vast majority (70%) of cells lacking BrdU staining contained two p220 foci, whereas 87% of BrdU-positive cells (in green) contained four p220 foci (in red) (Fig. 1d).

Consistent with the hypothesis of cell cycle-regulated foci formation, quantitative analysis of relative 4',6-diamidino-2-phenylindole (DAPI) signal intensity of 200 cells indicated that nuclear DNA content of normal human dermal fibroblasts with two or fewer foci was generally lower than that of cells with three or four foci (Fig. 2a). Thus, the majority of cells containing three or four foci appeared to have undergone at least partial DNA replication and were in S or G₂ phases. To substantiate this conclusion, we examined the status of p220 and DNA replication in cells stimulated to re-enter the cell cycle from quiescence (Fig. 2c). Normal dermal fibroblasts were pulsed-labeled with BrdU before harvest to mark S-phase cells. After 72 h of growth arrest (0 h), only one out of 100 cells scored was BrdU positive, and this cell had four p220 foci. In contrast, 81% of BrdU-negative cells had two foci, 15% had one or no focus, and 3% had three or four foci. At 12 h after release, 11% of the cells had entered S phase and were BrdU positive. Among these cells, 78% contained four p220 foci and 20% had three foci. Only 2% had two foci. In contrast, 90% of the BrdU-negative cells had two foci and 4% had one focus at this time point, whereas the balance had three or four foci. A similar pattern was observed for the 18- and 24-h time points, when 66% and 80% of cells were in S phase, respectively. At 48 h after release, 35% of the cells entered the second G₁ phase and became BrdU negative. Of these cells, 83% again contained only two p220 foci, and 7% had one or no focus, with the remainder containing three or four foci. We paid special attention to the small population of mitotic cells. p220 foci persisted in prophase (Fig. 3b, left panel, and top cell in the right panel), but they were absent by metaphase (Fig. 3b, middle panel) or telophase (Fig. 3b, right panel, bottom cell). The

Figure 1. p220 is located in cell cycle-regulated nuclear foci. (a) Affinity-purified polyclonal antibodies against p220 immunoprecipitate a closely spaced doublet of proteins 220 kD in molecular mass from tissue culture cells. For a large-scale immunoprecipitation, nuclear extracts from 293T cells (44 mg in 9 mL) were immunoprecipitated with 20 μ g of anti-p220 antibodies or pre-immune IgG bound to 80 μ L of protein A-Sepharose. Washed immunoprecipitates were separated using SDS-PAGE, and the gel was stained with Coomassie blue (*top*). A small fraction of this immune complex was immunoblotted with anti-p220 antibodies (*bottom*). (M) Molecular mass markers with masses indicated at left; (NRS) normal rabbit sera; (IP) immunoprecipitate. (b) p220 is localized in discrete nuclear foci. WI38 fibroblasts were subjected to indirect immunofluorescence using anti-p220 antibodies in the presence (*right*) or absence (*left*) of 0.5 μ g of antigen. (red) p220; (blue) nuclei stained with 4',6-diamidino-2-phenylindole (DAPI). (c) Cells with four p220 foci accumulate during S phase. Asynchronous bjtERT fibroblasts were pulse-labeled with BrdU for 60 min and then stained for p220 and BrdU. The number of p220 foci in BrdU-positive and BrdU-negative cells was determined from a minimum of 100 cells. (d) An example of BrdU-positive (green) cells displaying three or four p220 foci (red), whereas a BrdU-negative cell had two p220 foci. DAPI staining of nuclei is in blue.



loss of p220 foci during this short period would explain the small number of cells with one or no p220 focus (Fig. 2a). Taken together, these data demonstrate that the number of p220 foci is cell cycle regulated and that S phase is accompanied by the generation of two additional p220 foci not seen in G1 or G0 cells.

p220 foci are associated with CBs and with chromosomes 1 and 6

The size and number of p220 foci observed in S-phase cells are reminiscent of those displayed by CBs, as detected by antibodies against a component p80^{coilin}. CBs are present in variable numbers in tissue culture cell lines (three to eight CBs/cell) (Frey and Matera 1995; Almeida et al. 1998). Because CBs typically are difficult to detect in nontransformed cells, we used antigen retrieval to examine whether p220 might be associated with CBs in normal human dermal fibroblasts. As shown in Figure 3a, p220 foci coincide with coilin-containing CBs. In contrast to the colocalization of p220 and coilin throughout most of the cell cycle observed with three lines of fibroblasts (diploid dermal fibroblasts, WI38 lung fibroblasts, and bjtERT fibroblasts), transformed cells, including HeLa, Caski, SiHa, and MCF7 cells, displayed a larger and more variable number of p220 foci, ranging from three to >12 (data not shown). In HeLa cells, most if not all of the p220 foci are associated with CBs, but only a subset of CBs is associated with p220 foci (Fig. 3c).

Because CBs have previously been demonstrated to associate with histone gene clusters on chromosomes 1 and 6, it follows that one or more p220 foci may be expected to associate with these chromosomal domains. By using interphase chromosome painting in normal dermal fibroblasts, we found that chromosome 6 signals were closely associated with both p220 foci in 100% of cells containing two p220 foci. In 87% of cells containing four foci, the signals were associated with two foci, whereas the remaining 13% had more than two associated foci (Fig. 3d; Table 1). In contrast, chromosome 1 signals typically were not associated with p220 foci in cells containing two foci, but 93% of cells with four foci had two associated foci (Fig. 3e; Table 1). In our experience, false positive association occurs at a frequency of ~10% or lower. Because a subset of CBs is physically associated with an snRNA U2 gene loci at 17q21 (Frey and Matera 1995), we painted chromosome 17 as well as chromosomes 5 and Y as additional controls. These chromosomal domains displayed only rare association with p220 foci (Fig. 3e). For example, out of 400 cells, two were found to have one p220 focus associated with chromosome Y. Taken together, these data indicate that p220 foci are intimately linked with chromosome 1- and chromosome 6-associated CBs and that the chromosome 6 domain is associated with p220 foci throughout the cell cycle, whereas association with chromosome 1 occurs during S phase and coincides with the increase in p220 foci from two to four. These data also imply the exis-

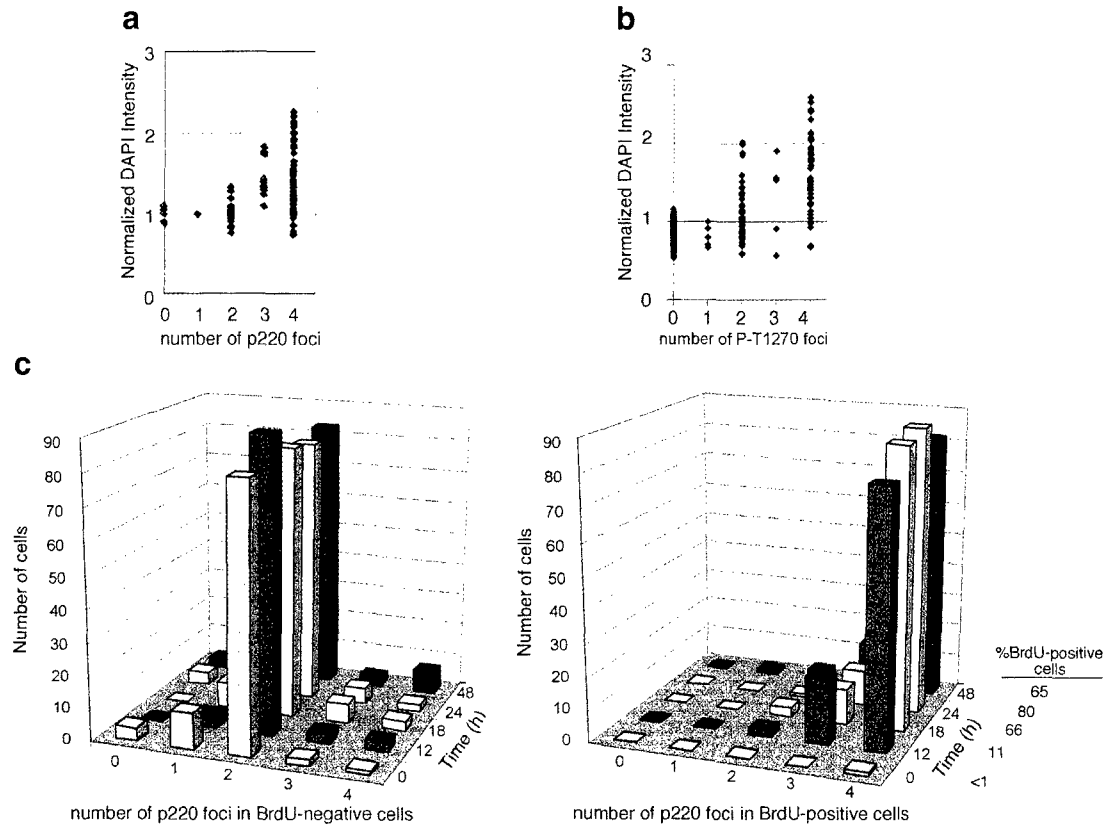


Figure 2. S-phase entry from quiescence is accompanied by the generation of four p220 foci in normal diploid fibroblasts. Quantification of nuclear DNA contents in human dermal fibroblasts containing different numbers of foci as detected with antibodies against p220 (a) or with an antibody against the phosphopeptide-spanning T1270 (b). Two hundred cells were analyzed for each experiment. (c) Quiescent normal dermal fibroblasts were stimulated to enter the cell cycle by serum addition. Cells were pulsed-labeled with BrdU at the indicated times before immunofluorescence to detect p220 and BrdU. The number of p220 foci was determined in 200 cells per time point, 100 each for BrdU-positive and BrdU-negative cells. [DAPI] 4',6-diamidino-2-phenylindole.

tence of mechanisms that restrict association of p220 with particular chromosomes to particular points in the cycle. The increased number of p220 foci observed in some transformed cells (data not shown) likely reflects at least in part an increased ploidy in chromosomes 1 and 6.

p220 is specifically phosphorylated by cyclin E/Cdk2 on sites near the cyclin E interaction domain

Cyclin E and p220 co-immunoprecipitate from cell extracts, and cyclin E/Cdk2 can phosphorylate associated p220 (Zhao et al. 1998). To elucidate the role of cyclin E/Cdk2 in p220 regulation, we sought to determine the specificity of phosphorylation. Initially we examined the ability of p220 to bind to various cyclin/Cdk complexes. Flag-tagged p220 was expressed in insect cells and cell lysates used in binding assays with immobilized cyclin/Cdk complexes (Fig. 4). Although p220 associated efficiently with the cyclin E/Cdk2 complex (lane 16), it did not associate with the cyclin D1/Cdk4, cyclin A/Cdk1, or cyclin B/Cdk1 complex (lanes 4, 10, and 13, respec-

tively) and bound only weakly with cyclin A/Cdk2 (lane 7). Thus, p220 displays specificity for cyclin E/Cdk2.

As expected, p220 was readily phosphorylated by the associated cyclin E/Cdk2 complex, and this phosphorylation was accompanied by reduced mobility of p220 (Fig. 4, lanes 16 and 17). Although p220 bound weakly to cyclin A/Cdk2, the associated protein underwent a similar mobility shift in the presence of ATP (lanes 7 and 8), suggesting that cyclin A/Cdk2 can also phosphorylate p220 when bound. We note that control reactions employing control insect cell lysates revealed the presence of a cyclin E/Cdk2-associated substrate (indicated by the asterisk) that migrated slightly faster than did p220 (Fig. 4, lanes 9 and 18). It can be distinguished from the human p220, because it was also phosphorylated to similar levels by cyclin A/Cdk2.

We next sought to determine the sites of p220 phosphorylation in vitro by using mass spectrometry (Zhang et al. 1998). p220 contains 18 potential Cdk phosphorylation sites (Thr/Ser followed by Pro). Four tryptic p220 phosphopeptides containing five phosphorylation sites were identified in recombinant p220 phosphorylated by

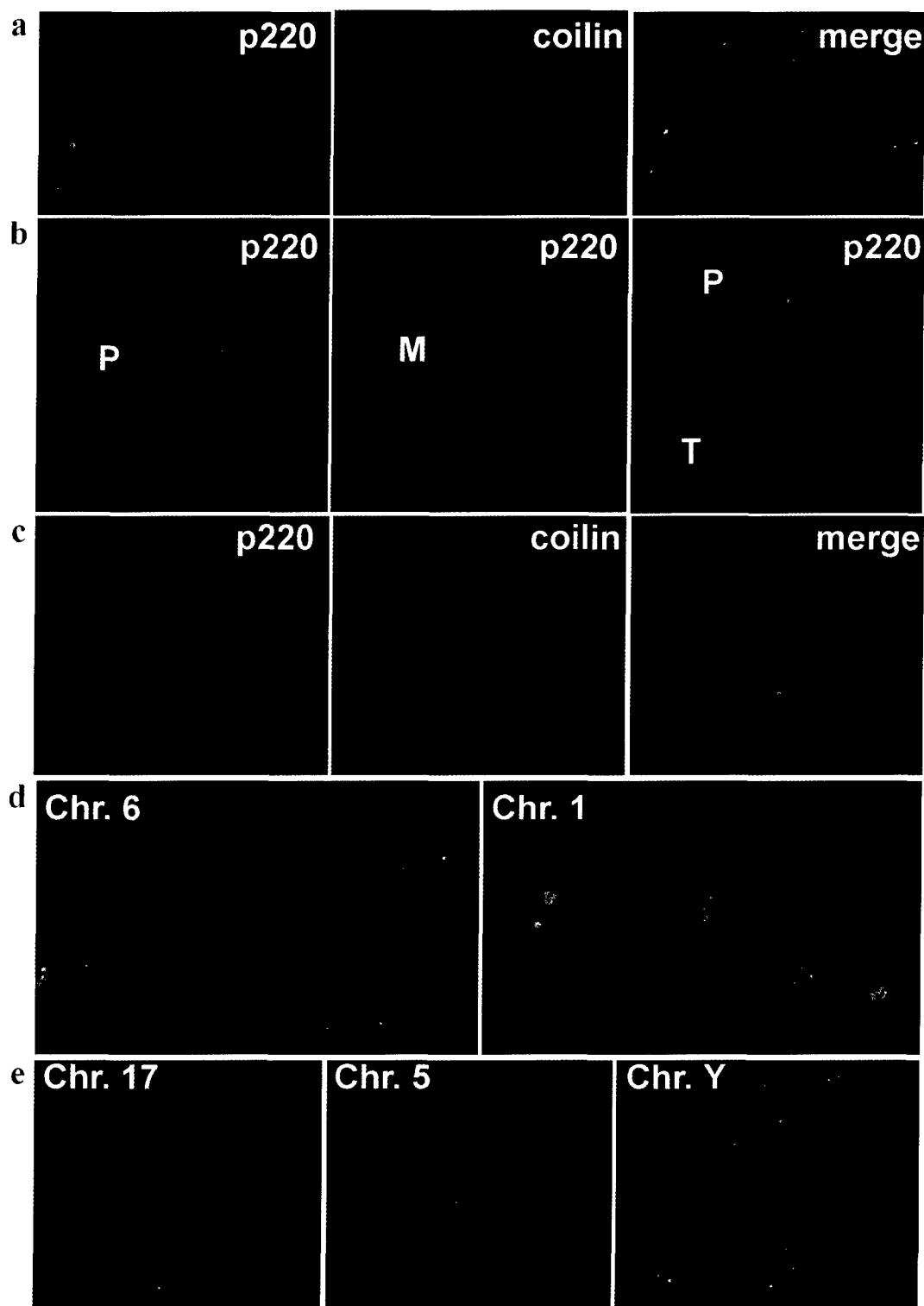


Figure 3. Association of p220 foci with Cajal bodies (CBs) and with domains of chromosomes 1 and 6. In all panels, 4',6-diamidino-2-phenylindole (DAPI) stained nuclear DNA blue. (a) Normal dermal fibroblasts were subjected to immunofluorescence by using anti-p220 (green) and anti-p80^{coilin} monoclonal antibodies (red) known to stain CBs. Co-localization is demonstrated in the merged image. (b) p220 foci are present in prophase (left; right, cell on top), but are no longer detectable in metaphase (middle) and telophase (right, cell at bottom). Prophase cells with four p220 foci were also observed (not shown). (c) HeLa cells contain CBs devoid of p220 foci. In a-c, p220 is green and DAPI is blue; in a and c, coilin is red. (d) and (e) p220 foci are associated with chromosomes 1 and 6 but not with other chromosomes. Normal dermal fibroblasts were stained for p220 and for the indicated chromosomal domains by using chromosome paints. For chromosomes 6, 17, 5, and Y, p220 is green and chromosome paint is red. For chromosome 1, p220 is red and chromosome paint green. (Chr.) Chromosome; (M) metaphase; (P) prophase; (T) telophase.

Table 1. Association of p220 foci with chromosomes 6 and 1

	No. of foci associated	Chromosome 6 (%)	Chromosome 1 (%)
Cells with 2 foci	0	0	91
	1	0	9
	2	100	0
Cells with 4 foci	0	0	0
	1	0	1
	2	87	93
	3	11	6
	4	2	0

One hundred cells with 2 and 4 foci, respectively, were counted for association with the indicated chromosomes. With chromosomes Y, 5, and 17, association was rare; for example, 2 of 400 cells displayed one p220 foci associated with chromosome Y.

associated cyclin E/Cdk2 in vitro (Fig. 5a,b; Table 2). Three singly phosphorylated peptides were sequenced by liquid chromatography/mass spectrometry/mass spectrometry (LC/MS/MS) to identify the phosphorylation sites as S1100 (site 3), T1270 (site 4), and T1350 (site 5), respectively (Table 2). The sequence of a doubly phosphorylated peptide encompassing residues 742–788 could not be determined because of its large size (*m/z* 5077.5, average mass; see Fig. 5a). However, this peptide contains two consensus Cdk substrates at S775 and S779 (sites 1 and 2) (Table 2), allowing a tentative assignment as sites of modification by cyclin E/Cdk2. Indeed, we found that p220 mutated in both of these serine residues was resistant to a cyclin E/Cdk2-induced shift in mobility (Fig. 5d). In contrast, p220 proteins mutated in one or more of the other identified phosphorylation sites still underwent a mobility shift in response to cyclin E/Cdk2 treatment (Fig. 5d). These data are consistent with the assignment of S775 and S779 as in vitro substrates and indicate that they are primarily responsible for the mo-

bility shift observed upon phosphorylation by cyclin E/Cdk2.

To examine phosphorylation in vivo, we purified p220 from a 293T cell nuclear lysate by using immunoprecipitation (Fig. 1a) and subjected it to mass spectral analysis. p220 is present at low levels in this cell line, and from 44 mg of nuclear extract, we obtained 200 ng of p220. We were able to identify one peptide with the mass expected for a doubly phosphorylated peptide spanning Val742–Lys788 whose quantity was consistent with the level of protein available for analysis (Fig. 5b; Table 2). Importantly, this peptide is absent from spectra after treatment with a phosphatase (Fig. 5b), indicating that S775 and S779 are phosphorylated in vivo. Signals for the three singly phosphorylated peptides observed in vitro were not evident, possibly because of the small amounts of material available for analysis.

p220 phosphopeptide antibodies recognize phosphorylated p220 in vitro and in vivo

To investigate T1270 and T1350 phosphorylation in vivo, we generated phospho-specific antibodies against these sites. These antibodies recognize Flag-p220 purified from insect cells only after phosphorylation with cyclin E/Cdk2 (Fig. 5e, lanes 5 and 6). To examine the specificity of these antibodies for reaction with p220, we bound either wild-type p220 or p220^{ΔCdk} (containing Ala substitutions at S775, S779, S1100, T1270, and T1350) to immobilized cyclin E/Cdk2 and incubated these complexes in the presence or absence of ATP (Fig. 5e). Both antibodies recognized phosphorylated p220 (lane 2) but did not recognize p220^{ΔCdk}. The two proteins were present at comparable levels based on anti-p220 immunoblotting (lanes 3 and 4). The low levels of reactivity toward the in vitro-translated p220 in the absence of added ATP likely reflect phosphorylation that occurred during

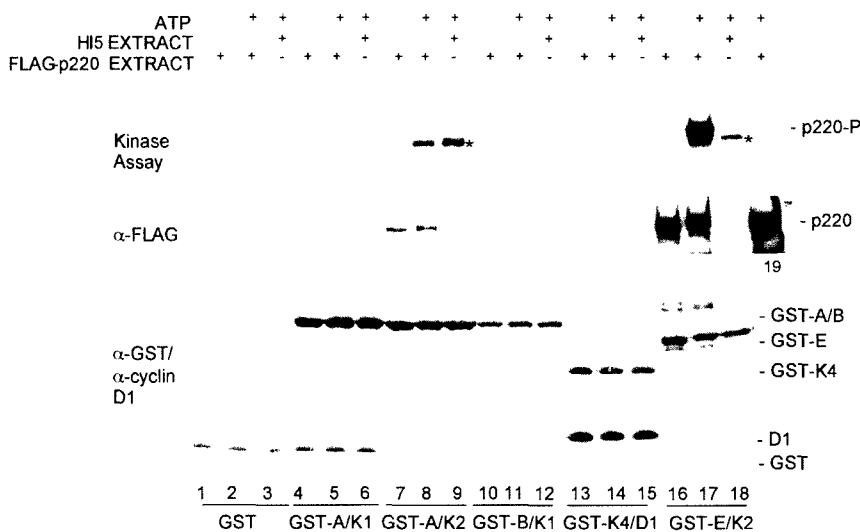
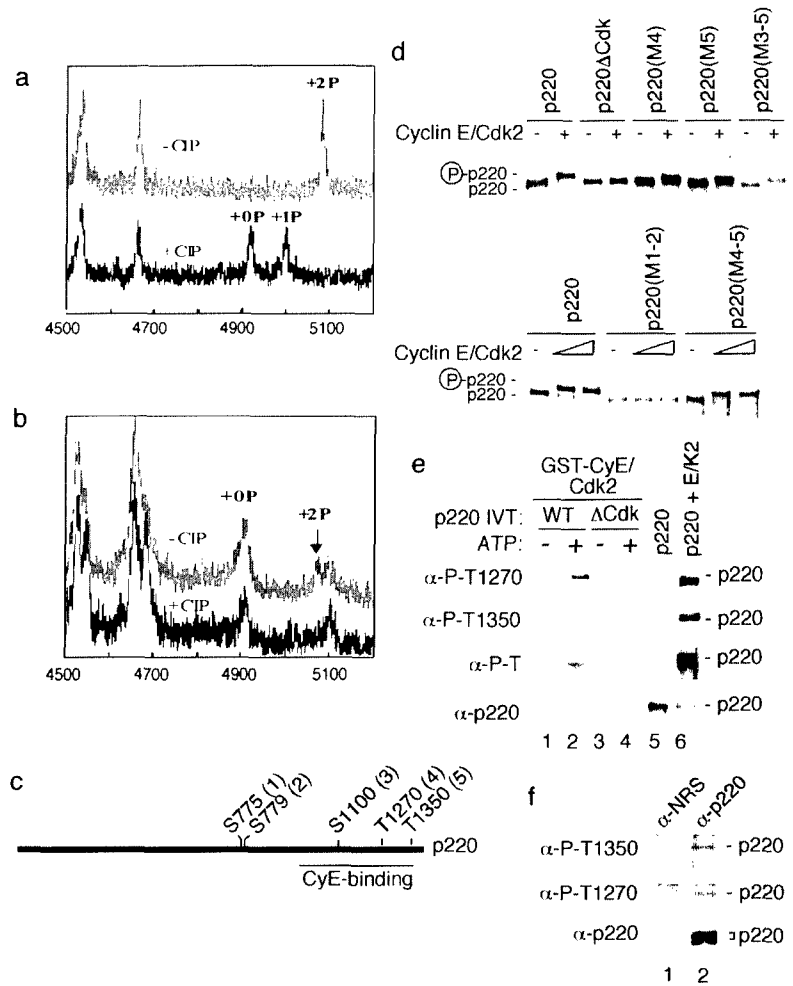


Figure 4. p220 preferentially associates with and is phosphorylated by cyclin E/Cdk2 in vitro. Immobilized cyclin/Cdk complexes were incubated with control insect cell lysates or insect cell lysates containing Flag-p220, as described in Materials and Methods. Complexes were washed with lysis buffer followed by 10 mM MgCl₂ and 20 mM Tris-HCl. Some samples were supplemented with γ -[³²P]ATP for 20 min before SDS-PAGE and visualization of proteins by immunoblotting or autoradiography. Flag-p220 was detected by anti-flag antibodies. The quantities of GST-cyclin/Cdk complexes were similar, as determined by immunoblotting with GST antibodies. Cdk2 complexes associated with an insect cell protein migrating slightly faster than p220 that was also a substrate for the kinase (indicated by an asterisk). An anti-flag immunoprecipitate of Flag-p220 (lane 19) was included as a control.

Figure 5. Identification of phosphorylation sites in p220. (a,b) A portion of the matrix-assisted laser desorption/ionization mass spectrometry (MALDI/TOF) mass spectra before (upper spectra) and after (lower spectra) treatment with calf intestinal phosphatase (CIP), showing the doubly phosphorylated peptide encompassing the sequence of 742–788 from recombinant (a) and endogenous (b) p220. To generate cyclin E/Cdk2–phosphorylated p220, 2 µg of Flag-p220 immobilized on anti-flag agarose was allowed to associate with 1 µg of cyclin E/Cdk2 and washed complexes incubated with 1 mM ATP (50 min at 25°C). (c) Schematic diagram of p220 phosphorylation sites and the cyclin E binding domain inferred by expression cloning (Zhao et al. 1998; Ma et al. 1999). (d) Altered mobility of p220 in response to cyclin E/Cdk2–mediated phosphorylation requires S775 and S779. In vitro translation products were incubated in the presence or absence of 20 nM cyclin E/Cdk2 for 20 min at 30°C (top) or with 20 and 50 nM cyclin E/Cdk2 for 20 min at 30°C (bottom) before electrophoresis and autoradiography. (e) Specificity of phosphopeptide-specific antibodies. In vitro–translated p220 or p220^{ΔCdk} (50 µL) was incubated with 1 µg of GST–cyclin E/Cdk2 immobilized on GSH-Sepharose, and washed complexes were incubated in the presence or absence of 1 mM ATP [lanes 1–4]. Proteins were separated by SDS–PAGE and immunoblotted. The anti-phosphoThr antibody (New England Biolabs), which reacts with a large number of different phosphoThr-Pro-containing sequences, did not recognize p220^{ΔCdk}. As a control, Flag-p220 from insect cells (~100 ng) was incubated with or without 50 nM cyclin E/Cdk2 and 1 mM ATP before immunoblotting. (WT) Wild type. (f) Anti-p220 immune complexes from 293T cells were separated by SDS–PAGE and immunoblotted with the indicated antibodies. (NRS) Normal rabbit serum.



immunoprecipitation from ATP-containing reticulocyte lysates, because larger amounts of recombinant p220 purified from insect cells did not react with the phosphopeptide-specific antibodies in the absence of phosphorylation by cyclin E/Cdk2 (lanes 5 and 6). We also note that a general phosphothreonine-proline antibody gave similar results, indicating that other TP sequences in

p220^{ΔCdk} are not phosphorylated by bound cyclin E/Cdk2 in vitro. We found that both phosphopeptide antibodies reacted with p220 immunoprecipitated from cycling 293T cells (Fig. 5f), indicating that these sites are indeed phosphorylated in vivo. On the basis of the comparison with p220 in 293T cells examined in parallel (Fig. 5f), the more slowly migrating p220 protein

Table 2. Mass spectral identification of p220 phosphorylation sites

Sites	Peptides	Molecular mass (measured/calculated)	No. of PO ₃ group
In vitro			
S775, S779	⁷⁴² V I I S D D P F V S S D T E L T S A V S S I N G E N L P T I L S S P T K S P T K N A E L V K ⁷⁸⁸	4918/4916.5	2
S1100	¹⁰⁹¹ N A V S F P N L D S P N V S S T L K P P S N N A I K ¹¹¹⁶	2712/2713.0	1
T1270	¹²⁵⁹ L A D S S D L P V P R T P G S G A G E K ¹²⁷⁸	1708/1707.9	1
T1350	¹³⁴⁶ T T S A T P L K D N T Q Q F R ¹³⁶⁰	1954/1954.1	1
In vivo			
S775, S779	⁷⁴² V I I S D D P F V S S D T E L T S A V S S I N G E N L P T I L S S P T K S P T K N A E L V K ⁷⁸⁸	4918/4916.5	2

Average molecular masses of dephosphorylated peptides are shown.

was preferentially detected by the phosphopeptide antibodies.

CB-associated p220 co-localizes with cyclin E and is phosphorylated on Cdk sites in a cell cycle-dependent manner

The data described thus far suggest that p220 is targeted to CBs and is a substrate of cyclin E/Cdk2. However, it is unclear whether p220 is phosphorylated while in CBs. To examine whether CB-associated p220 is phosphorylated on Cdk sites, we performed immunofluorescence by using antibodies against phospho-T1270 and phospho-T1350. Both recognized nuclear foci similar to the antibody against p220 (Fig. 6a; data not shown). To demonstrate that the foci coincided with those found with anti-p220, we performed double immunofluorescence staining with antibodies against phospho-T1270 and coilin in cycling fibroblasts (Fig. 6). From 500 cells scored, 30.2% displayed primarily two foci reactive toward both antibodies, whereas 40.4% had primarily four co-localized foci (Fig. 6a), including cells in prophase (Fig. 6b). The remaining 29.4% of the cells lacked staining with the phospho-T1270 antibody. This is in marked contrast to staining with p220 antibodies in which cells lacking

antibody reactivity were very rare except for those in metaphase and telophase (Figs. 2a and 3b). In cells that were negative for reactivity with anti-phospho-T1270, coilin reactivity was still observed (Fig. 6a). Quantification of relative DAPI intensity of 200 additional cells demonstrated that cells nonreactive with the phosphopeptide antibodies had a lower DNA content than did reactive cells, which is consistent with these cells being in the G1 phase, whereas phospho-T1270 antibody-positive cells had a higher DNA content consistent with S- or G2-phase cells (Fig. 2b). In this separate experiment, a somewhat higher percentage of cells had no detectable focus (data not shown). In agreement with the results with p220 antibodies, the few cells in metaphase and telophase were negative for staining with the phosphopeptide antibody, whereas coilin signals appeared dispersed (Fig. 6d,e).

If cyclin E is responsible for phosphorylation of p220 within CBs, one would predict that p220 would co-localize with cyclin E and that the timing of p220 phosphorylation would be coincident with co-localization. To examine this issue directly, we initially performed co-localization experiments using anti-cyclin E and anti-p220 antibodies. As shown in Figure 7a, cyclin E was concentrated in foci that are coincident with p220 foci. At

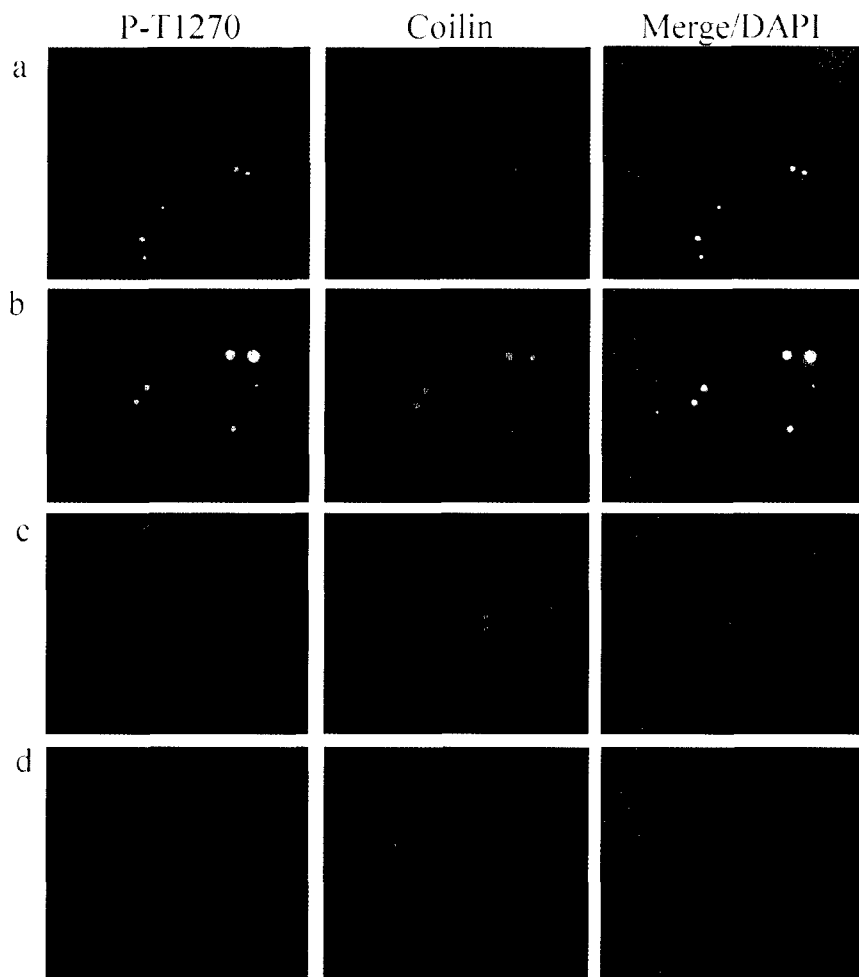


Figure 6. p220 in Cajal bodies (CBs) is phosphorylated on Cdk sites in a cell cycle-specific manner. Dual detection with anti-phospho-T1270 antibodies and p80^{coilin} in dermal fibroblasts is shown. Focal co-localization was observed in S phase (a) and prophase (b), but anti-phospho-T1270 did not detect any foci in metaphase (c) or telophase (d). a also contains three cells that display anti-coilin reactive foci but not anti-phospho-T1270 reactive foci. The DNA content of these cells is consistent with G1 phase (Fig. 2b). Only diffused coilin signals were observed in c and d. (Green) anti-phospho-T1270; (red) anti-coilin; (blue) 4',6-diamidino-2-phenylindole (DAPI).

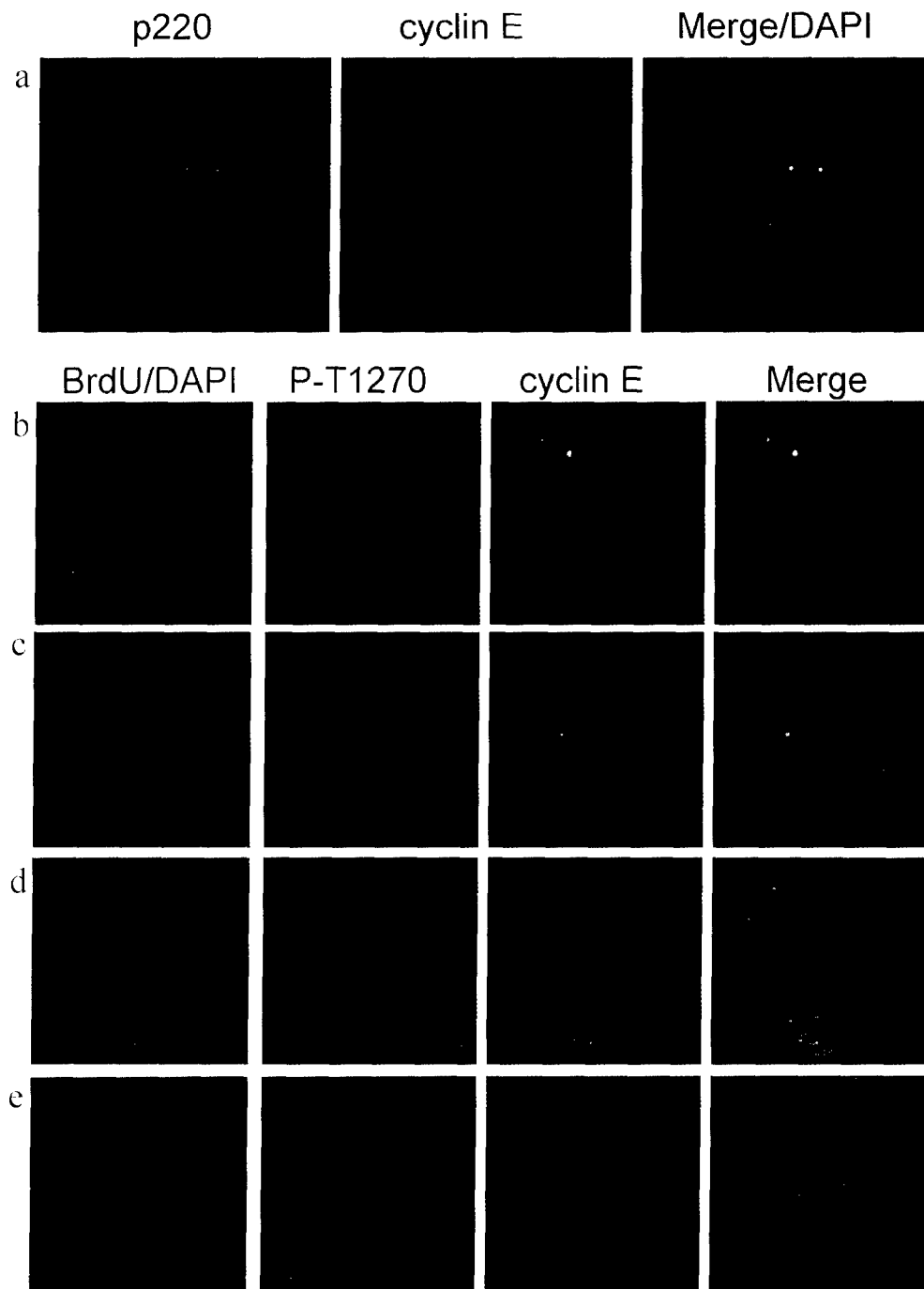


Figure 7. Co-localization of cyclin E with anti-phospho-T1270 reactive foci in a cell cycle-dependent manner. (a) Cyclin E (red) co-localizes with p220 (green) in a cell containing four p220 foci. Nuclei are in blue. (b–e) Growing diploid fibroblasts were labeled with BrdU for 1 h and subjected to immunofluorescence using anti-phospho-T1270 (red), anti-cyclin E (green), anti-BrdU (magenta), and 4',6-diamidino-2-phenylindole (DAPI; blue) to visualize nuclei. (b) A BrdU-negative cell containing two phospho-T1270 foci that co-localize with cyclin E. This field also contains a BrdU-negative cell that is negative for both anti-cyclin E and anti-phospho-T1270 antibodies. (c) A BrdU-positive cell containing two phospho-T1270 foci that co-localize with cyclin E adjacent to a BrdU-negative cell that is negative for both anti-cyclin E and anti-phospho-T1270 antibodies. (d) BrdU-positive cells containing two or four phospho-T1270 foci that co-localize with cyclin E. (e) A BrdU-negative cell containing four phospho-T1270 foci that lacks cyclin E staining.

longer exposure, cyclin E was evident as faint dust throughout the nucleus as well. These results are consistent with the recent report that cyclin E is concentrated in CBs in S phase (Lui et al. 2000).

To examine whether phosphorylation of p220 correlates with co-localization with cyclin E, we pulse-labeled asynchronous diploid fibroblasts with BrdU and determined the presence of phospho-T1270, cyclin E, BrdU,

and DAPI-stained nuclei (Fig. 7b–e). Among cells containing two phospho-T1270 foci, both BrdU-positive and BrdU-negative cells were observed; in both cases, however, these foci contained cyclin E (Fig. 7b–d). In contrast, among cells containing four anti-phospho-T1270 foci, those that were BrdU positive most frequently displayed co-localized cyclin E, whereas those that were BrdU negative typically lacked cyclin E staining (Fig. 7d,e). Given the data presented previously, we believe the latter class of cells to be G2 cells that have lost cyclin E expression but maintain p220 in a phosphorylated form.

The in situ results with antibodies to p220, phospho-T1270, phospho-T1350, coilin, and cyclin E (Figs. 1–3, 6; Liu et al. 2000) indicate the following: (1) p220 is an in vivo Cdk2 substrate and can be phosphorylated on cyclin E/Cdk2 sites while present in CBs. There is a tight correlation between the appearance of cyclin E in foci and the occurrence of p220 phosphorylation such that (2) cells that are nonreactive with antibody to phospho-T1270 are in the early G1 phase before cyclin E/Cdk2 is present to phosphorylate p220 in CBs. Consistent with this, cells that lacked anti-phospho-T1270 foci also lacked detectable cyclin E. (3) Cells containing two anti-phospho-T1270 reactive foci that co-localize with coilin and cyclin E are in late G1 or early S phases when cyclin E/Cdk2 levels peak. (4) Cells that have four co-localized foci are well into S phase, and p220 remains phosphorylated (Figs. 1 and 2). Although the pattern of p220 phosphorylation persists into prophase, cyclin E staining is lost at some point in late S phase or G2 phase, as exemplified by the presence of BrdU-negative cells containing four phospho-p220 foci but lacking cyclin E co-localization. (5) Around the time of metaphase and later, p220 foci are not detected with either p220 or phospho-T1270 antibodies.

Mutation of cyclin E/Cdk2 sites in p220 reduces p220-mediated histone H2B promoter activation

Our data suggest that cyclin E/Cdk2 may regulate p220 during the G1/S-phase transition. To examine this question, we took advantage of the recent finding that p220 expression in tissue culture cells leads to increased expression of histone 2B (H2B) promoter- and histone 4 (H4) promoter-luciferase reporter constructs, independent of its effects on S-phase acceleration (Zhao et al. 2000). Histone gene expression is complex, involving both message stabilization (approximately sevenfold) and transcriptional activation (approximately fivefold), which together account for an ~35-fold increase in histone mRNA levels during S phase (Harris et al. 1991; Heintz 1991). But the process by which the histone transcriptional apparatus senses cell cycle position is unknown.

We compared the ability of a vector expressing p220 (pCMV-p220) or p220^{ΔCdk} (pCMV-p220^{ΔCdk}) to activate luciferase expression from an H2B (-200/0) promoter-luciferase reporter plasmid in transiently transfected 293T cells (Fig. 8a). The level of induction by p220 rela-

tive to control transfections ranged from two- to 10-fold, depending on the quantity of p220 plasmid used and the level of p220 expression achieved, as determined by immunoblotting (Fig. 8b). In contrast, p220^{ΔCdk} displayed a substantially reduced ability to activate the H2B reporter construct when expressed at comparable levels (Fig. 8a–c). Similar results were obtained with a minimal H2B promoter (-127/-27) (data not shown). At low levels of expression, p220^{ΔCdk} displayed levels of H2B reporter activation comparable to control transfected cells (Fig. 8a,b); however, at higher levels of expression, a twofold increase in reporter activity over control transfected cells was typically observed (Fig. 8c,d). Transfected cells displayed p220 foci as well as diffuse signals throughout the nucleoplasm because of elevated levels of expression from the transfected plasmids (Fig. 8c). Taken together, these results suggest that phosphorylation at one or more cyclin E/Cdk2 sites contributes substantially to this aspect of p220 function. However, it is possible that elevated levels of p220 can partially bypass a requirement for phosphorylation at these sites. In these experiments, p220 appeared to be primarily in a more slowly migrating phosphorylated form, while p220^{ΔCdk} remained in a more rapidly migrating form (Fig. 8b,d). Thus, it appeared that sufficient cyclin E/Cdk2 existed in these cells to phosphorylate fully the transiently expressed p220. This may explain why co-expression of cyclin E/Cdk2 had little effect on the levels of H2B promoter activity in 293T cells (data not shown).

Consistent with a role for cyclin E/Cdk2-mediated phosphorylation in p220 function, we found that co-expression of p57^{KIP2}, which can inhibit Cdk2 activity and block cells at the G1/S-phase transition (Matsuoka et al. 1995), led to a reduction in the ability of p220 to activate H2B promoter activity in transiently transfected cells (Fig. 8f). In this experiment, the levels of p220 expression plasmid used were such that a twofold increase in H2B promoter activity was observed, but p57^{KIP2} reduced luciferase levels below that obtained with control transfected cells. As expected, expression of p57^{KIP2} alone also reduced the levels of promoter activity in the absence of p220 expression (Fig. 8f). This repression likely reflects the fact that cells are blocked in G1 with low cyclin E/Cdk2 activity. Immunoblotting demonstrated comparable levels of expression of p220 and p220^{ΔCdk} and verified the expression of p57^{KIP2} (data not shown).

S-phase entry in quiescent fibroblasts by cyclin E/Cdk2 expression is associated with the accumulation of four p220 foci

Expression of cyclin E/Cdk in quiescent fibroblasts leads to S-phase entry (Connell-Crowley et al. 1998; Leone et al. 1998). Because the appearance of four p220 foci is associated with S phase in asynchronous and serum-stimulated cells (Figs. 1 and 2), we wondered whether S-phase entry by an alternative mechanism would also lead to the appearance of four p220 foci. To this end, quiescent WI38 cells were stimulated to enter the cell cycle by infection with adenoviruses (Ad) expressing cyc-

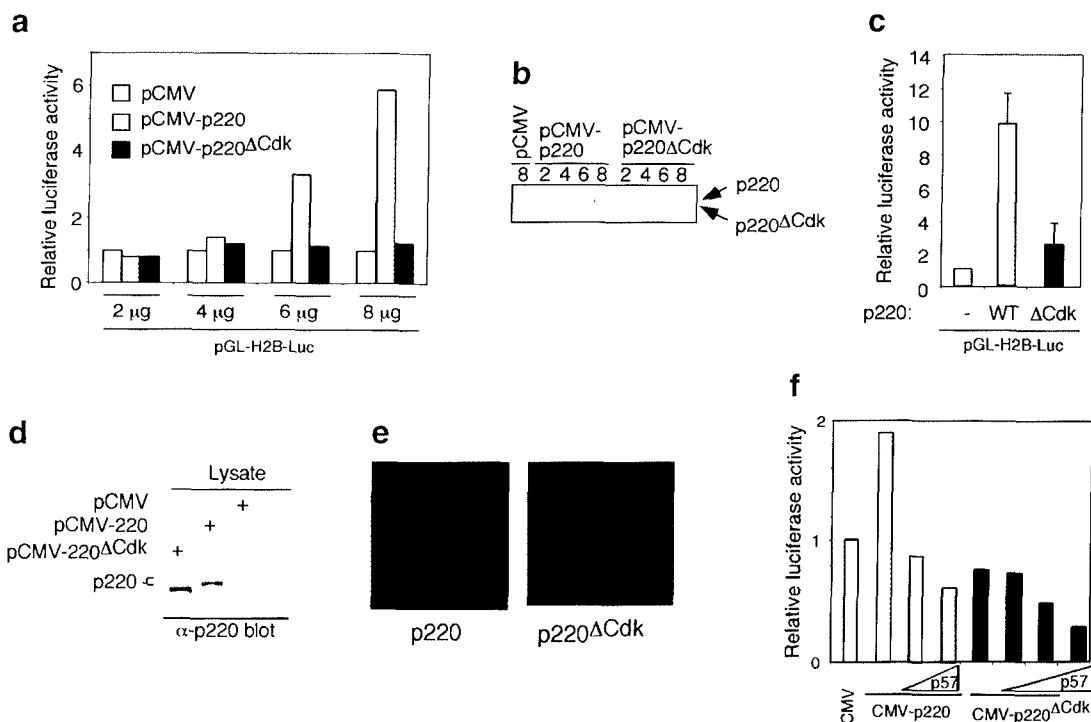


Figure 8. Cyclin E/Cdk2-mediated phosphorylation of p220 is important for optimal p220-induced histone H2B transcriptional activation. (a) pCMV, pCMV-p220, or pCMV-p220 Δ Cdk was transfected into 293T cells (3.5-cm dish), along with 50 ng of pCMV- β -galactosidase and 50 ng of pGL-H2B-luciferase reporter plasmid, and subsequently processes for luciferase and β -galactosidase activity as described in Materials and Methods. Luciferase activities were normalized relative to β -galactosidase activities. (b) A portion of extracts used in a was immunoblotted using anti-p220 antibodies. The wild-type p220 protein comigrates with the endogenous protein found at low levels, whereas p220 Δ Cdk migrates slightly faster as a result of the absence of phosphorylation. (c) The results of two independent experiments each performed using triplicate independent calcium phosphate precipitates derived from 10 μ g of pCMV, pCMV-p220, or pCMV-p220 Δ Cdk are shown. (-) Lacking p220; (WT) wild type. (d) and (e) Expression levels for p220 and p220 Δ Cdk for experiments shown in c were similar as determined by immunoblotting (d) or immunofluorescence (e). (f) Expression of p57^{K112} blocks activation of the H2B promoter by p220 overexpression. 293T cells were transfected with limiting amounts of pCMV-p220 or p220 Δ Cdk expressing plasmids (5 μ g) in the presence or absence of either 1 or 2 μ g of pCMV-p57^{K112}. At this level of expression, p220 leads to a twofold increase in reporter activity. p57^{K112} expression leads to a dramatic reduction in the level of p220-induced reporter activity in the presence or absence of p220 expression. The averages of duplicate independent transfections are shown.

clin E and Cdk2. At 24 h after infection, cells were pulse-labeled with BrdU for 1 h before analysis of p220 by immunofluorescence. BrdU-negative cells in control cultures maintained in low serum contained predominantly two p220 foci (Fig. 9a,b). In contrast, a large fraction of BrdU-positive cells in the cyclin E/Cdk2-treated culture contained four foci, whereas BrdU-negative cells in the culture contained predominantly two foci. These results suggest that cyclin E/Cdk2 can function upstream of the pathway responsible for the establishment of four p220 foci during S phase.

Discussion

Cell cycle transitions are driven in part by transcriptional programs that generate proteins needed for subsequent processes. Although it is clear that these transcriptional programs are ultimately linked to the basic cell cycle machinery, how this linkage is accomplished is largely unknown. The best understood connection between transcription and the basic cell cycle machinery in mammalian cells is the activation of E2F by Cdk-

mediated phosphorylation of Rb family members (Dyson 1998; Nevins 1998). In this article, we provide evidence, at the cellular and molecular level, that cyclin E/Cdk2 directly regulates the activity of p220^{N¹A¹T}, which in turn controls S-phase-specific activation of histone gene transcription. Thus, cyclin E/Cdk2 not only regulates the production of DNA synthesis machinery through E2F but also supports the production of nucleosome components required for completion of DNA replication.

In normal fibroblasts, p220 is localized to discrete foci in the nucleus, and the number of these foci change during the cell cycle (Zhao et al. 2000; this work). Cells in G1 contain primarily two p220 foci, whereas cells in S phase contain four foci. Anti-p220-reactive foci are only absent during the short span of metaphase and telophase (Figs. 2, 3, and 6). These p220 foci coincide with small nuclear organelles, the CBs (Fig. 3). CBs contain a bewildering number of transcriptional and splicing/polyadenylation proteins, and recent studies have led to the hypothesis that CBs function as sites of assembly of pol II transcriptosomes, complexes of pol II transcription fac-

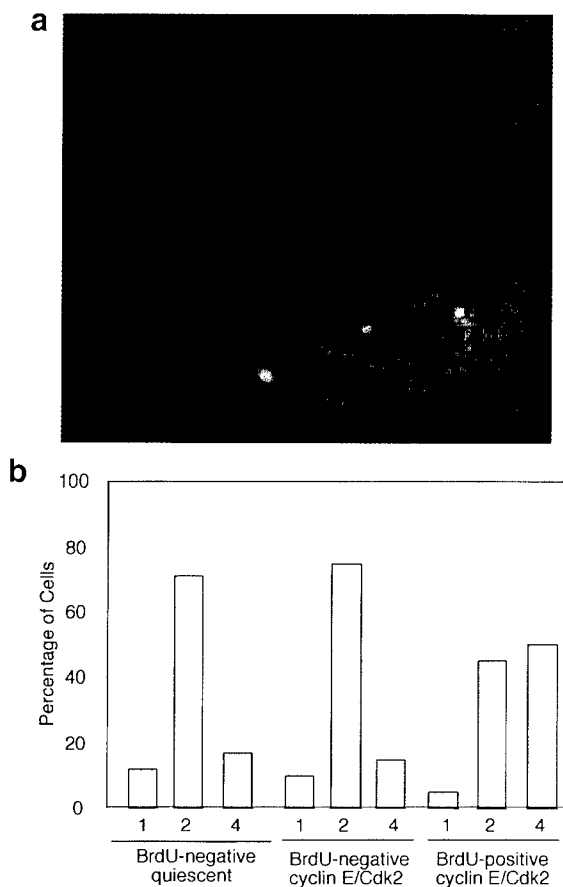


Figure 9. S-phase entry in quiescent fibroblasts by cyclin E/Cdk2 expression is associated with the appearance of four p220 foci. WI38 fibroblasts were subjected to serum deprivation for 72 h before infection with Ad-cyclin E/Cdk2 and maintained in 0.1% serum. Twenty-four h after infection, cells were pulse-labeled with BrdU for 1 h before analysis of p220 staining by immunofluorescence. (a) An example of an S-phase cell from a cyclin E/Cdk2 infection containing four p220 foci adjacent to a non-S-phase cell containing two p220 foci. (b) Quantitation of p220 foci. Thirty to 100 nuclei of each class were counted.

tors and splicing machinery (Gall et al. 1999). CBs also contain specialized proteins such as histone stem-loop binding proteins that function in the processing of histone 3' ends (Abbott et al. 1999). In addition, cyclin E/Cdk2 is present in CBs during S phase (Liu et al. 2000). Although it was suggested that this localization of cyclin E/Cdk2 reflects the presence of the Cdk-activating kinase cyclin H/Cdk7 in coiled bodies, our results suggest that cyclin E/Cdk2 plays an S-phase-promoting role within CBs, at least in part by phosphorylating p220.

An interesting aspect of CBs is their physical attachment to discrete gene loci. In HeLa cells, a subset of CBs co-localize with replication-dependent histone gene clusters on chromosomes 1 and 6 (1q21 and 6p21, respectively) and with snRNA genes located elsewhere in the genome (Frey and Matera 1995). Our results indicate that p220-containing CBs associate with the chromosome 6 domain during G1 and S/G2 and additionally with the chromosome 1 domain during S phase and G2, but we

found little evidence for association with the domains of chromosomes 5, 17, or Y (Fig. 3). Typically, the p220 foci linked with chromosome 6 appeared to be larger than those associated with chromosome 1 (Fig. 3), potentially reflecting the larger numbers of histone genes located in the chromosome 6 cluster. The cell cycle-dependent association of p220 with CBs on chromosomes 6 and 1 then accounts for the oscillation in p220 foci numbers. Zhao et al. (2000) have also demonstrated that p220 is localized with chromosomes 1 and 6 and have shown that p220 is physically linked to histone gene loci.

On a biochemical level, p220 preferentially binds to cyclin E/Cdk2 over other Cdk complexes and is phosphorylated by cyclin E/Cdk2 *in vitro* and *in vivo* (Figs. 4 and 5). Indeed p220 foci also contain cyclin E (Fig. 7). Moreover, antibodies specific to p220 (Figs. 1–3) and to specific phosphopeptides of p220 (Figs. 6 and 7) demonstrated that p220 is present in CBs in both Cdk2 phosphorylated form and unphosphorylated forms and that these two forms alternate during the cell cycle. Three major classes of staining patterns were observed with phospho-specific antibodies against p220. Thirty percent of cells in an asynchronous population lacked phospho-T1270 antibody reactivity and displayed predominantly a G1 DNA content while maintaining detectable CBs. Because the vast majority of G1 cells contain two p220 foci co-localized with CBs (Figs. 1 and 2), we conclude that p220 in a distinct population of G1 cells is not phosphorylated on Cdk2 sites. This population of cells also lacked cyclin E staining, which is consistent with these cells being in early G1. Cells in the second class (30%) contain two phospho-T1270 antibody reactive foci that are co-localized with cyclin E. Our analysis indicates that these cells are in either late G1 or early S phase and suggests that chromosome 6-associated p220 can be phosphorylated on Cdk2 sites in advance of the formation of four obvious foci. In asynchronous cells, a small fraction of BrdU-positive cells have two clear p220 foci (Fig. 1c), suggesting that S phase can be initiated before the accumulation of p220 in chromosome 1-associated CBs. This idea is substantiated by the finding that some cells containing two anti-phospho-T1270 and anti-cyclin E reactive foci display partial replication, as determined by quantitation of DNA content or BrdU incorporation (Figs. 2b and 7). However, we cannot rule out the possibility that p220 is already present in chromosome 1-associated CBs but is present at levels below detection. Cells in a third class (40%) each contained four phospho-antibody reactive foci, and a substantial fraction of these cells contained co-localized cyclin E. These cells have a higher DNA content, consistent with p220 being phosphorylated in S and G2. p220 phosphorylation is maintained in prophase, with some cells displaying two foci and some displaying four foci, but p220 foci are absent in metaphase and telophase. Thus, p220 foci appear to be lost sequentially during the prophase-to-metaphase transition. The fate of p220 during mitosis is unclear at present. It could be dispersed and therefore beyond our means to detect at this stage in the cycle. Alternatively, p220 could be degraded. Consistent with

the latter possibility is the finding that 293T cell extracts from mitotic cells (obtained by mitotic shake-off) have no detectable p220 by immunoprecipitation/immunoblotting analysis (data not shown). Thus, if p220 is degraded in mitosis, new p220 must be synthesized early in G1 phase and be incorporated into CBs in the unphosphorylated form before the activation of cyclin E/Cdk2 at late G1 and early S phase. In HeLa cells released from mitosis, p220 foci and coilin foci reappear 2–3 h after release, consistent with the formation of foci in early G1 phase (data not shown).

The link between p220, a cyclin E/Cdk2 interacting protein (Zhao et al. 1998; Ma et al. 1999), and the transcription of histone 2B and histone 4 genes (Zhao et al. 2000) led us to address whether cyclin E/Cdk2 directly regulates this aspect of p220 function. In principle, cyclin E/Cdk2 could function to relay cell cycle positional information to p220, thereby playing a role in controlling the timing of S-phase-specific histone gene transcription. We found that p220 lacking five Cdk2 phosphorylation sites, four of which were phosphorylated *in vivo*, displayed a reduced ability to activate transcription from an H2B reporter construct (Fig. 8), consistent with a role for cyclin E/Cdk2 in p220 activation and H2B transcription. p220-dependent activation of the H2B promoter requires the Oct-1 element (data not shown) known to be involved in S-phase-specific induction of H2B expression (Fletcher et al. 1987; Segil et al. 1991). Using a U2OS-based tissue culture system, Zhao et al. (2000) found that the ability of p220 to activate H4 transcription was stimulated by co-expression of cyclin E, again pointing to a role for cyclin E in this process. Although we did not observe a stimulatory effect of cyclin E/Cdk2 co-expression in our system, we found that the vast majority of ectopic p220 in 293T cells is in the slower mobility phosphorylated form (Fig. 8), suggesting that cyclin E is not a limiting component in these cells at the levels produced with our p220 expression plasmid. Apparently, at the levels of expression achieved in U2OS cells, cyclin E/Cdk2 is limiting. Regardless of these differences, both studies indicate that the cyclin E/Cdk2-mediated, cell cycle-dependent activation of p220 is an important component of the S-phase-specific histone transcriptional program.

Although cyclin E/Cdk2 activation seems to be central to p220 function, several issues remain to be addressed. First, what is the significance of p220 localization in CBs? Although p220 is clearly localized in these organelles and these organelles are physically linked to target genes, it is conceivable that the localization of p220 reflects its accumulation before release from CBs in a form that then activates histone gene transcription. Many transcription factors accumulate in inactive pools and are not present in detectable levels at target gene loci. Nevertheless, the co-localization of p220 with cyclin E, CBs, and histone gene clusters, the cell cycle-dependent phosphorylation of p220, the persistent association of phosphorylated p220 with CBs throughout S phase when histone genes are transcribed, as well as the activation of histone gene transcription by Cdk2-dependent p220

phosphorylation are most striking and strongly point to a functional role for p220 and cyclin E localization in CBs, as summarized in Figure 10. Second, what is the basis of the appearance of p220 foci on chromosome 1 during S phase, and how is this regulated? Presumably, the association of p220 foci with chromosome 1 reflects a role in S-phase-dependent histone transcription, but why then do p220 foci exist on chromosome 6 throughout most of the cell cycle? In this regard, it is important to determine whether transcription from endogenous histone genes is linked to accumulation of p220 at histone gene clusters. Third, the histone gene cluster on chromosome 6 contains >50 copies of the four classes of core histones as well as the linker histone H1 (Ahn and Gruen 1999). Does p220 coordinately regulate the transcription of all classes of histone genes in the locus, and if so, how is this achieved? One possibility is that p220 could generate a chromosomal context that allows transcriptional activation of the whole region during S phase. If this is the case, p220 might also regulate the expression of nearby genes during S phase. Analysis of the 6p21 region reveals a large number of nonhistone genes, and it is possible that one or more of these genes are under the control of a p220-dependent S-phase transcriptional program. Alternately, p220 might function within the CB to assemble histone-specific transcription complexes, in keeping with the proposed function of CBs (Gall et al. 1999). Fourth, although p220 overexpression increases the S-phase population in transiently transfected cells (Zhao et al. 1998), it remains to be determined whether this activity is related to histone transcription and whether the phosphorylation events that we have identified are relevant to this activity. Finally, the finding that cyclin E is concentrated in CBs suggests the possibility that these organelles are important control centers linking the cell cycle machinery to S-phase-specific pro-

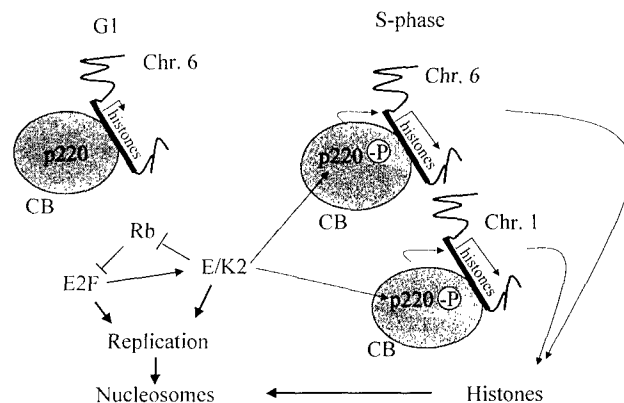


Figure 10. Summary and proposed model of cell cycle-dependent transcriptional activation of histone genes on chromosomes 1 and 6 in association with Cajal bodies (CBs) as mediated by cyclin E/Cdk2 phosphorylation of p220. p220 foci are no longer detectable by metaphase and telophase but reappear in G1 phase. However, phosphorylation of p220 in CBs does not occur until cyclin E/Cdk2 is activated during late G1 phase/S phase.

cesses. It will therefore be important to determine whether other relevant cyclin E substrates gain access to the kinase through localization in CBs.

Materials and methods

Cell culture

Normal diploid fibroblasts (dermal fibroblasts, WI38, and bJERT), 293T, and HeLa cells were maintained in Dulbecco's modified Eagle's medium (DMEM) supplemented with 10% fetal bovine serum (FBS). To generate quiescent fibroblasts, cells were plated at ~50% confluence before culture for 72 h without serum. Cells were released into DMEM containing 10% FBS for various lengths of time. In some experiments, the cells were exposed to BrdU (10–50 µg/mL) for 1 h before harvest to reveal cells in S phase. To examine cell cycle entry via cyclin E/Cdk2 expression, WI38 cells were maintained for 72 h in 0.1% FBS and infected with adenoviruses expressing cyclin E and Cdk2 (generously provided by J. Nevins, Duke University, Durham, NC) (Leone et al. 1998) at a multiplicity of infection of 100.

Antibodies and immunofluorescence assays

Bacterial GST-p220 (residues 1054–1397) was used to generate antibodies in rabbits. Antibodies were depleted of reactivity to the GST protein and affinity-purified using immobilized GST-p220. Anti-coilin monoclonal antibodies (π -isotype) were provided by M. Carmo-Fonseca (University of Lisbon, Portugal; Almeida et al. 1998). Anti-cyclin E (HE12) came from Pharmingen. Antibodies against Thr-1270 (Asp-Leu-Pro-Val-Pro-Arg-phosphoThr-Pro-Gly-Ser-Gly-Ala-Gly-Cys) and Thr-1350 (Ser-Arg-Thr-Thr-Ser-Ala-phosphoThr-Pro-Leu-Lys-Asp-Asn-Thr-Cys) were generated in rabbits after coupling to keyhole limpet hemocyanin. For immunofluorescence, cells were fixed in either ethanol or formalin and permeabilized with 0.1% Triton X-100. Detection of rabbit antibodies was accomplished using secondary antibodies labeled with Cy3 or Alexa 488 (Molecular Probes, Eugene, OR) or with anti-rabbit horseradish peroxidase (HRP) (Roche, Indianapolis, IN) and tyramides (NEN, Boston, MA) (see below). BrdU was detected using fluorescein isothiocyanate (FITC)-conjugated anti-BrdU antibody. Nuclear DNA was revealed with DAPI staining. Microscopic analysis was performed using either an Olympus BX-60 fitted with an Optronics CCD camera (Baylor College of Medicine) or an AX-70 Olympus microscope and an Olymix digital camera (University of Alabama). Images were captured with a 100× objective lens by using either multiband pass filters or single pass filters with merging using Adobe Photoshop.

Correlation of p220 foci or phospho-T1270 foci with DNA content

Asynchronous human dermal fibroblasts were fixed with 4% paraformaldehyde, permeabilized with 0.5% Triton X-100 in phosphate-buffered saline (PBS), and then treated with 3% hydrogen peroxide. Slides were then incubated with a 1:100 dilution of anti-p220 or anti-phosphopeptide for 2 h at 37°C and washed three times in PBS containing 0.1% Tween 20. After incubation with anti-rabbit HRP (1:100), cells were washed three times, and the signals were developed using a 1:100 dilution of cyanine-3-tyramide (NEN). To detect BrdU, the cells were fixed once more with 4% paraformaldehyde, treated with 3 N HCl for 15 min, incubated with an anti-BrdU FITC antibody

for 2 h at 37°C, DAPI (Sigma) stained, and mounted with anti-fade.

Relative nuclear DNA content was determined as follows: After staining with various antibodies, we took images of DAPI and of the p220 or phosphopeptide foci separately, but all images came from the same slide to avoid any variability in DAPI staining. Using Image Pro Plus software (Media Cybernetics, Silver Spring, MD), we identified nuclei to be measured and determined the average DAPI density individually. The average background for each image was then determined and subtracted, giving the corrected average nuclear DAPI density for each cell. Cells were then individually correlated to the foci number. For graphic representation (Fig. 2a,b), the average DAPI density of all two-foci nuclei (the majority of which were BrdU negative; see Figs. 1 and 2c) was used to divide the density of each individual cell. This normalization procedure yielded a number between 1 (G1) and 2 (G2) and somewhere in between (S).

Interphase chromosome painting

Asynchronous primary human dermal fibroblasts were fixed and stained with antibodies to p220, and signals were developed with tyramide as described above. Slides were fixed again with 4% paraformaldehyde and treated with RNase A (100 µg/mL) in 2 × SSC (1 × SSC is 0.15 M NaCl and 0.015 M sodium citrate) for 1 h at 37°C. They were then ethanol-dehydrated and denatured in 70% formamide, 2 × SSC, pH 7.0, for 2 min at 72°C, dehydrated in ethanol, and hybridized individually with chromosome paints overnight at 37°C. The chromosome 1 and chromosome Y paints were a direct FITC conjugate or cyanine 3 conjugate, respectively, from Vysis (Downers Grove, IL). Signals were detected according to the manufacturer's protocol. Paints for chromosome 5, 6, or 17 were digoxigenin probes from Oncor (Gaithersburg, MD). They were detected using an anti-dig Texas Red antibody. The slides were DAPI stained before imaging.

Immunoprecipitation and phosphorylation

For nuclear extracts, 293T cells were lysed in 50 mM Tris-HCl, pH 7.5, containing 1 mM EDTA, 100 mM NaCl, 0.3% Nonidet P-40, and protease/phosphatase inhibitors, and nuclei pelleted by centrifugation. Nuclear proteins were solubilized using RIPA buffer (50 mM Tris-HCl at pH 7.5, 150 mM NaCl, 0.5% deoxycholate, 1% Nonidet P-40, 0.1% SDS, and protease/phosphatase inhibitors) before centrifugation. Extracts were precleared with protein A-bound normal rabbit IgG before incubation with affinity-purified anti-p220 antibodies bound to protein A-Sepharose. Beads were washed with RIPA buffer. Proteins were separated by SDS-PAGE before staining with Coomassie Brilliant Blue R 250 or transferred to nitrocellulose filters for immunoblotting with anti-p220 antibodies. Detection was accomplished using enhanced chemiluminescence (Amersham).

For expression of p220 in insect cells, the coding sequence (Imai et al. 1996) was cloned into pUNI-50, and in vitro recombination was then used to generate a pVL1392-based plasmid with p220 fused at its N terminus to the Flag tag as described (Liu et al. 1998). Viruses were made using Baculogold (Pharmingen). To examine interaction with Cdks, cyclin/Cdk complexes were purified with glutathione-Sepharose beads (Ma et al. 1999). Immobilized complexes were then incubated with insect cell extracts with or without Flag-p220. Complexes were washed with lysis buffer and with 20 mM Tris-HCl, pH 7.5, and 10 mM MgCl₂. A portion of each mixture was used for kinase assays employing 50 µM γ -[³²P]ATP. Samples were separated by

SDS-PAGE and transferred to nitrocellulose before immunoblotting and autoradiography.

Matrix-assisted laser desorption/ionization mass spectrometry (MALDI/TOF) with delayed extraction (Voyager-DE, Perceptive Biosystems, Framingham, MA) was used for the identification of phosphopeptides, as described by Zhang et al. (1998). An electrospray ion trap mass spectrometer (LCQ, Finnigan, San Jose, CA) coupled on-line with a capillary high-pressure liquid chromatograph (Magic 2002, Auburn, CA) was used for identification of phosphorylation sites. A MAGICMS C18 column (5 μ m particle diameter, 150 \AA pore size, 0.1 \times 50 mm dimension) was used for the LC/MS/MS analysis.

Plasmids and reporter assays

Mutations were generated using a Gene Editor kit (Promega). Mutated and wild-type p220 coding sequences were cloned into pcDNA3.1 for expression. To generate histone gene reporter plasmids, H2B regulatory sequences (-200/0 or -127/-27) were cloned into the luciferase reporter pGL3 (Promega). To examine histone transcription, pCMV-p220, pGL3 reporter plasmids, and pCMV- β -galactosidase plasmids were co-transfected into 293T cells at 50%–80% confluence by using calcium phosphate. Twenty-four h after precipitate removal, extracts were generated and normalized for β -galactosidase activity before measurement of luciferase activity.

Acknowledgments

We thank J. Gall for discussions, J. Zhao, A.G. Matera, and E. Harlow for communicating results before publication, M. Carmo-Fonseca for anti-coilin antibodies, and Richard Atkinson, Brian Streib, and Heather Benedict-Hamilton for assistance. J.W.H. was supported by U.S. Public Health Service (USPHS) grant GM54137 and by the Welch Foundation. L.T.C. was supported by USPHS grants CA36200 and DE/CA11910. B.A.V.T. was partially supported by the University of Alabama Medical Scientist Training Program. The Digital Imaging Microscopy Facility at the University of Alabama was supported by the University of Alabama Health Services Foundation and by grant DE/CA11901.

The publication costs of this article were defrayed in part by payment of page charges. This article must therefore be hereby marked "advertisement" in accordance with 18 USC section 1734 solely to indicate this fact.

References

- Abbott, J., Marzluff, W.F., and Gall, J.G. 1999. The stem-loop binding protein (SLBP1) is present in coiled bodies of the *Xenopus* germinal vesicle. *Mol. Biol. Cell.* **10**: 487–499.
- Adams, P.D., Sellers, W.R., Sharma, S.K., Wu, A.D., Nalin, C.M., and Kaelin, W.G., Jr. 1996. Identification of a cyclin-cdk2 recognition motif present in substrates and p21-like cyclin-dependent kinase inhibitors. *Mol. Cell. Biol.* **16**: 6623–6633.
- Ahn, J. and Gruen, J.R. 1999. The genomic organization of the histone clusters on human 6p21.3. *Mamm. Genome* **10**: 768–770.
- Almeida, F., Saffrich, R., Ansorge, W., and Carmo-Fonseca, M. 1998. Microinjection of anti-coilin antibodies affects the structure of coiled bodies. *J. Cell Biol.* **142**: 899–912.
- Brown, N.R., Noble, M.E., Endicott, J.A., and Johnson, L.N. 1999. The structural basis for specificity of substrate and recruitment peptides for cyclin-dependent kinases. *Nat. Cell Biol.* **1**: 438–443.
- Cajal, S.R.Y. 1903. Un sencillo metodo de coloracion seletiva del reticulo protoplasmatico y sus efectos en los diversos organos nerviosos de vertebrados e invertebrados. *Trab. Lab. Invest. Biol.* **2**: 129–221.
- Connell-Crowley, L., Elledge, S.J., and Harper, J.W. 1998. G1 cyclin-dependent kinases are sufficient to initiate DNA synthesis in quiescent human fibroblasts. *Curr. Biol.* **8**: 65–68.
- Di Fruscio, M., Weiher, H., Vanderhyden, B.C., Imai, T., Shiomi, T., Hori, T.A., Jaenisch, R., and Gray, D.A. 1997. Proviral inactivation of the Npat gene of Mpv 20 mice results in early embryonic arrest. *Mol. Cell. Biol.* **17**: 4080–4086.
- Dulic, V., Lees, E., and Reed, S.L. 1992. Association of human cyclin E with a periodic G1-S phase protein kinase. *Science* **257**: 1958–1961.
- Dyson, N. 1998. The regulation of E2F by pRb-family proteins. *Genes & Dev.* **12**: 2245–2262.
- Fletcher, C., Heintz, N., and Roeder, R.G. 1987. Purification and characterization of OTF-1, a transcription factor regulating cell cycle expression of a human histone H2b gene. *Cell* **51**: 773–781.
- Frey, M.R. and Matera, A.G. 1995. Coiled bodies contain U7 small nuclear RNA and associate with specific DNA sequences in interphase human cells. *Proc. Natl. Acad. Sci.* **92**: 5915–5919.
- Gall, J.G., Bellini, M., Wu, Z., and Murphy, C. 1999. Assembly of the nuclear transcription and processing machinery: Cajal bodies (coiled bodies) and transcriptosomes. *Mol. Biol. Cell.* **10**: 4385–4402.
- Harris, M.E., Bohni, R., Schneiderman, M.H., Ramamurthy, L., Schumperli, D., and Marzluff, W.F. 1991. Regulation of histone mRNA in the unperturbed cell cycle: Evidence suggesting control at two posttranscriptional steps. *Mol. Cell. Biol.* **11**: 2416–2424.
- Heintz, N. 1991. The regulation of histone gene expression during the cell cycle. *Biochim. Biophys. Acta* **1088**: 327–339.
- Imai, T., Yamauchi, M., Seki, N., Sugawara, T., Saito, T., Matsuda, Y., Ito, H., Nagase, T., Nomura, N., and Hori, T. 1996. Identification and characterization of a new gene physically linked to the ATM gene. *Genome Res.* **6**: 439–447.
- Koff, A., Giordano, A., Desai, D., Yamashita, K., Harper, J.W., Elledge, S.J., Nishimoto, T., Morgan, D.O., Franza, B.R., and Roberts, J.M. 1992. Formation and activation of a cyclin E-cdk2 complex during the G1 phase of the human cell cycle. *Science* **257**: 1689–1694.
- Leng, X., Connell-Crowley, L., Goodrich, D., and Harper, J.W. 1997. S-phase entry upon ectopic expression of G1 cyclin-dependent kinases in the absence of retinoblastoma protein phosphorylation. *Curr. Biol.* **7**: 709–712.
- Leone, G., DeGregori, J., Jakoi, L., Cook, J.G., and Nevins, J.R. 1998. Collaborative role of E2F transcriptional activity and G1 cyclin-dependent kinase activity in the induction of S phase. *Proc. Natl. Acad. Sci.* **96**: 6626–6631.
- Liu, J., Hebert, M.D., Ye, Y., Templeton, D.J., Kung, H., and Matera, A.G. 2000. Cell cycle-dependent localization of the CDK2-cyclin E complex in Cajal (coiled) bodies. *J. Cell Sci.* **113**: 1543–1552.
- Liu, Q., Li, M.Z., Leibham, D., Cortez, D., and Elledge, S.J. 1998. The univector plasmid-fusion system, a method for rapid construction of recombinant DNA without restriction enzymes. *Curr. Biol.* **8**: 1300–1309.
- Lukas, J., Herzinger, T., Hansen, K., Moroni, M.C., Resnitzky, D., Helin, I., Reed, S.I., and Bartek, J. 1997. Cyclin E-induced S phase without activation of the Rb/E2F pathway. *Genes & Dev.* **11**: 1479–1492.
- Ma, T., Zou, N., Lin, B.Y., Chow, L.T., and Harper, J.W. 1999. Interaction between cyclin-dependent kinases and human

- papillomavirus replication-initiation protein E1 is required for efficient viral replication. *Proc. Natl. Acad. Sci.* **96**: 382–387.
- Matsuoka, S., Edwards, M.C., Bai, C., Parker, S., Zhang, P., Baldini, A., Harper, J.W., and Elledge, S.J. 1995. p57KIP2, a structurally distinct member of the p21CIP1 Cdk inhibitor family, is a candidate tumor suppressor gene. *Genes & Dev.* **9**: 650–662.
- Nevins, J.R. 1998. Toward an understanding of the functional complexity of the E2F and retinoblastoma families. *Cell Growth Differ.* **9**: 585–593.
- Ohtsubo, M., Theodoras, A.M., Schumacher, J., Roberts, J.M., and Pagano, M. 1995. Human cyclin E, a nuclear protein essential for the G1-to-S phase transition. *Mol. Cell. Biol.* **15**: 2612–2624.
- Reed, S.I. 1997. Control of the G1/S transition. *Cancer Surv.* **29**: 7–23.
- Russo, A.A., Jeffrey, P.D., Patten, A.K., Massague, J., and Pavletich, N.P. 1996. Crystal structure of the p27Kip1 cyclin-dependent-kinase inhibitor bound to the cyclin A-Cdk2 complex. *Nature* **382**: 325–331.
- Schulman, B.A., Lindstrom, D.L., and Harlow, E. 1998. Substrate recruitment to cyclin-dependent kinase 2 by a multi-purpose docking site on cyclin A. *Proc. Natl. Acad. Sci.* **95**: 10453–10458.
- Segil, N., Roberts, S.B., and Heintz, N. 1991. Mitotic phosphorylation of the Oct-1 homeodomain and regulation of Oct-1 DNA binding activity. *Science* **254**: 1814–1816.
- Sherr, C.J. 1996. Cancer cell cycles. *Science* **274**: 1672–1677.
- Zhang, X., Herring, C.J., Romano, P.R., Szczepanowska, J., Brezeska, H., Hinnebusch, A.G., and Qin, J. 1998. Identification of phosphorylation sites in proteins separated by polyacrylamide gel electrophoresis. *Anal. Chem.* **70**: 2050–2059.
- Zhao, J., Dynlacht, B.D., Imai, T., Hori, T., and Harlow, E. 1998. Expression of NPAT, a novel substrate of cyclin E-CDK2, promotes S-phase entry. *Genes & Dev.* **12**: 456–461.
- Zhao, J., Kennedy, B.K., Lawrence, B.D., Barbie, D., Matera, A.G., Fletcher, J.A., and Harlow, E. 2000. NPAT links cyclin E-cdk2 to the regulation of replication-dependent histone gene transcription. *Genes & Dev.* **14**: 2283–2297 (this issue).
- Zhu, L., Harlow, E., and Dynlacht, B.D. 1995. p107 uses a p21CIP1-related domain to bind cyclin/cdk2 and regulate interactions with E2F. *Genes & Dev.* **9**: 1740–1752.

Loss of Heterozygosity Events Impeding Breast Cancer Metastasis Contain the *MTA1* Gene¹

Michelle D. Martin, Kathy Fischbach, C. Kent Osborne, Syed K. Mohsin, D. Craig Allred, and Peter O'Connell²

Breast Center [M. D. M., C. K. O., S. K. M., D. C. A., P. O.], Departments of Molecular and Cellular Biology [M. D. M., P. O.], Medicine [C. K. O.], and Pathology [S. K. M., D. C. A.], Baylor College of Medicine, Houston, Texas 77030, and Department of Life Sciences, University of Texas at San Antonio, San Antonio, Texas 78249 [K. F.]

Abstract

Breast cancer mortality is seldom attributable to the primary tumor, but rather to the presence of systemic (metastatic) disease. Axillary lymph node dissection can identify the presence of metastatic breast cancer cells and serves as a marker for systemic disease. Previous work in our laboratory determined that rates of loss of heterozygosity (LOH) of a 1.6-Mb region of chromosome 14q 31.2 is much higher in axillary lymph node-negative primary breast tumors than in axillary lymph node-positive primary breast tumors (P. O'Connell *et al.*, *J. Natl. Cancer Inst.*, 91: 1391-1397, 1999.). This unusual observation suggests that, whereas the LOH of this region promotes primary breast cancer formation, some gene(s) mapping to this 1.6-Mb region is rate-limiting for breast cancer metastasis. Thus, if primary breast cancers delete this region, their ability to metastasize decreases. To identify this gene(s), we have physically mapped this area of chromosome 14q, confirmed the position of two known genes and 13 other expressed sequence tags into this 1.6-Mb region. One of these, the metastasis-associated 1 (*MTA1*) gene, previously identified as a metastasis-promoting gene (Y. Toh *et al.*, *J. Biol. Chem.*, 269: 22958-22963, 1994.), mapped to the center of our 1.6-Mb target region. Thus, *MTA1* represents a strong candidate for this breast cancer metastasis-promoting gene.

Introduction

One of the strongest prognostic factors for cancer-free survival after treatment of the primary tumor is the presence or absence of local metastatic spread. For women with axillary lymph node-negative breast cancer, 90% survive more than 5 years after diagnosis. This is compared with a 70% 5-year survival for women with axillary lymph node-positive disease, and only a 20% 5-year survival for women with distant metastases (1). The development of the metastatic phenotype of a tumor cell involves a complicated series of events that include detachment of tumor cells from the primary tumor, invasion into and survival in the circulatory and lymphatic systems, extravasation, and induction of angiogenesis and growth at the metastatic site. The development of a genetic test that could predict the metastatic potential of a primary breast tumor would increase the effectiveness of breast cancer treatment.

Previous work in our laboratory involved LOH³ analysis to compare DNA samples from paired normal and breast tumor tissues to examine whether specific genetic changes in primary breast cancer can serve as markers of metastatic potential (2). As expected, increas-

ing rates of LOH were correlated with progressively higher stages of breast cancer (3, 4). Unlike all other 14 markers tested, LOH at marker D14S62 was much lower in metastases than in primary breast tumors. D14S62 LOH proved to be associated with node-negative primary cancers and thus with slower spread to distant sites. Higher resolution LOH studies narrowed this phenomenon to a 1.6-Mb region near marker D14S62 (2). Here we have assembled a physical map and identified a minimum tiling path of three YAC clones that span this region. One of the ESTs that mapped into this region in our study was *MTA1*, a gene previously shown to be highly expressed in both metastatic breast cancer cell lines and metastatic gastrointestinal carcinomas (5, 6).

Materials and Methods

YAC DNA Preparation and Mapping. CEPH YACs were selected for mapping of *MTA1* by screening with D14S62 region markers or on the basis of available mapping information.⁴ Total YAC DNA from each clone was purified as described previously (4). Each YAC clone was confirmed by PCR analysis using oligonucleotide primers for *MTA1* and selected ESTs mapping into the region on the basis of the radiation hybrid mapping of chromosome 14 (Gene Map 1999 and the GDB). The primers used were a *MTA1*-expressed sequence tag (RH78599) designed by the Sanger Center and based on known human genomic chromosome 14 sequence.⁵ The primer sequences were 5'GGTTCGGATTGGCTTGTA3', which is contained within a unique sequence of the *MTA1* cDNA; and 5'CGTGGTTCTGGACAAGGG3', which is contained in the adjacent genomic sequence of *MTA1*. PCR was performed in a Gene Amp PCR system 9600 (Perkin-Elmer Corp., Norwalk, CT) using ~20 ng of YAC DNA in a volume of 50 μ l in 30 cycles at 94°C for 30 s, 56°C for 30 s, and 72°C for 30 s. A 20- μ l volume of each product was electrophoresed in a 1% agarose gel, and PCR products were visualized by ethidium bromide staining.

BAC DNA Preparation and Mapping Analysis. BAC 76E12 was obtained from Research Genetics (Birmingham, AL). Total BAC DNA was purified according to the protocol supplied by the manufacturer. *MTA1* was mapped to BAC 76E12 by PCR analysis using the same oligonucleotide primers for *MTA1* as above. PCR was performed in a Gene Amp PCR system 9600 (Perkin-Elmer Corp.) using ~30 ng of BAC DNA in a volume of 50 μ l in 30 cycles at 94°C for 30 s, 56°C for 30 s, and 72°C for 30 s. A 10- μ l volume of each product was electrophoresed in a 1% agarose gel, and PCR products were visualized by ethidium bromide staining.

Results

As part of our preliminary mapping studies of the region, we determined all of the ESTs that mapped into the target region according to the radiation hybrid-based NCBI Gene Map. A total of 12 ESTs, but no known genes, map to this 1.6-Mb metastasis-related region. However, we performed additional mapping analysis on the YACs used in the preliminary mapping analysis and confirmed two known genes and 13 ESTs that actually map to these YACs, rather than their location indicated by the radiation hybrid-based NCBI Gene

Received 1/25/01; accepted 3/14/01.

The costs of publication of this article were defrayed in part by the payment of page charges. This article must therefore be hereby marked *advertisement* in accordance with 18 U.S.C. Section 1734 solely to indicate this fact.

¹ Supported by CA58183 and CA30195 from the National Cancer Institute, NIH, Department of Human Services.

² To whom requests for reprints should be addressed, at Breast Center, Baylor College of Medicine, One Baylor Plaza, MS600, Houston, Texas 77030. Phone: (713) 798-1631; Fax: (713) 798-1659; E-mail: poconnell@breastcenter.tmc.edu.

³ The abbreviations used are: LOH, loss of heterozygosity; *MTA1*, metastasis-associated 1; EST, expressed sequence tags; NCBI, National Center for Biotechnology Information; GDB, Genome Database; YAC, yeast artificial chromosome; BAC, bacterial artificial chromosome.

⁴ For example, Internet address: <http://www-genome.wi.mit.edu>; <http://www.gdb.org>.

⁵ Internet address: <http://www.sanger.ac.uk>.

Map. Because of these findings, we included the region from marker D14S1066 to the telomere of chromosome 14 because of uncertainties inherent in radiation hybrid mapping to insure that we had complete coverage of the telomeric end of chromosome 14q. Approximately 392 ESTs map into this region, with 63 of these being previously identified genes. Table 1 summarizes the known genes in the region from D14S1066 to the telomere (including *MTA1*) considered to be possible metastasis candidate genes.

MTA1 had been mapped previously using radiation hybrids onto the NCBI Gene Map some distance away from our region of interest near the telomere of chromosome 14q. We had, however, discovered several ESTs thought to map elsewhere on chromosome 14 that were actually mapped to our target region. Because *MTA1* represented a promising candidate gene even though the gene map showed it to be outside our target region, we then tested PCR primers for the *MTA1* gene onto our physical map of the region detected by our LOH studies. We determined *MTA1* mapped onto YACs 859d4 and 765h7 (Fig. 1). These mapping studies were subsequently confirmed when we mapped the gene onto BAC 76E12, which has a completed draft sequence that confirms its mapping onto YAC 859d4. The *MTA1* gene was therefore determined to map onto chromosome 14q in the vicinity of markers D14S62 and D14S51, or ~21 cM proximal to its previously reported location (see Fig. 1). Fig. 2, A and B, summarizes the gel-mapping data for *MTA1*. *MTA1* was mapped onto the overlap-

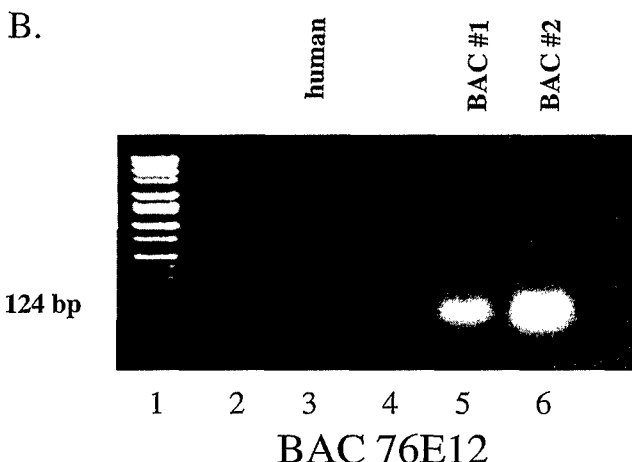
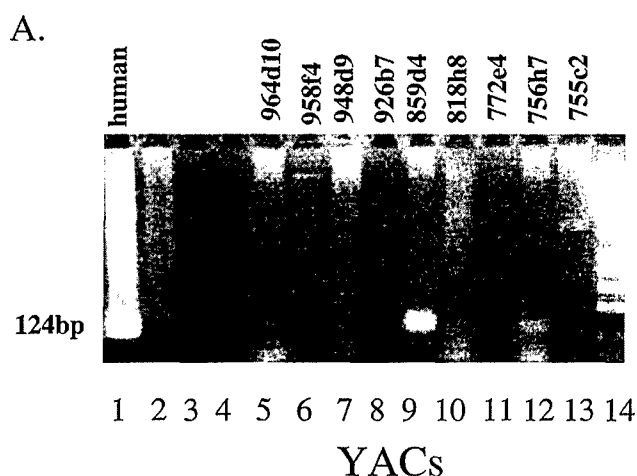


Fig. 2. Gel-mapping data on *MTA1*. A, PCR amplification of *MTA1* primers on YAC clones spanning the metastasis gene target region (band shown in Lanes 1, 9, and 12). Positive control was provided with 25 ng of human genomic DNA shown in Lane 1. B, PCR amplification of *MTA1* primers on BAC clone 76E12. Two positives are shown in Lanes 5 and 6 that represent two different preparations of the same BAC. Twenty-five ng of human genomic DNA was once again used as a positive control (Lane 3). Product size in both experiments was ~124 bp.

ping YAC clones 859d4 and 756h7. Fig. 2B indicates that *MTA1* also maps to BAC 76E12, and its location to this sequenced BAC clone is confirmed by a BLAST search with *MTA1* cDNA sequences.

Discussion

MTA1 was previously identified as a metastasis-promoting gene overexpressed in both rat and human metastatic cell lines (5). The human *MTA1* gene was cloned and sequenced by Nawa *et al.* (7) in 2000. In 1994, the rat gene was cloned and sequenced by the same group (5). The expression of *MTA1* in the human breast cancer cell line MDA-MB-231, a metastatic cell line, was determined to be approximately four times higher than its expression levels in the breast cancer cell line MDA-MB-468, which is nonmetastatic (5). The rat cell lines MTC.4, a benign line that remains phenotypically stable with prolonged passage, and the highly metastatic line MTLn3 were also tested for expression of *mta1* (the rat homologue). The expression level of *mta1* was found to be 4-fold higher in the MTLn3 line than in the MTC.4 line by Northern blotting (8). Different forms of cancer have also been shown to overexpress *MTA1*. Esophageal, colorectal, gastric, and pancreatic carcinomas have all been reported previously to express higher levels of *MTA1* mRNA than paired normal tissues, and this overexpression correlated with the invasiveness or lymph node metastasis of each of the carcinomas (6, 9, 10).

Table 1 Possible candidate genes in the 14q region of interest

Nineteen known genes were determined to map into the area of interest on chromosome 14. Both the gene name and the GDB no. are given for identification.^a

Gene name	GDB no.
<i>CALM</i> , calmodulin 1	9611304
<i>PRSC1</i> , protease, cysteine, 1	700617
<i>CGHA</i> , chromogranin A	119777
<i>PI</i> , protease inhibitor 1	120289
<i>AACT</i> , α -1-antichymotrypsin	118955
<i>PCI</i> , protein C inhibitor	134739
<i>TCL1A</i> , T-cell leukemia/lymphoma 1A	250785
<i>CCNK</i> , cyclin K	9957298
<i>YY1</i> , YY1 transcription factor	216988
<i>CKB</i> , creatine kinase, brain	120590
<i>AKT1</i> , V-akt murine thymoma viral oncogene	118989
<i>EIF5</i> , eukaryotic translation initiation factor 5	126411
<i>IGHG3</i> , immunoglobulin- γ 3	119339
<i>MTA1</i> , metastasis-associated 1	9955068
<i>MARK3</i> , MAP/microtubule affinity-regulating kinase	9315109
<i>EMAP1</i> , echinoderm microtubule-associated protein	6328385
<i>KNS2</i> , kinesin 2	304673
<i>TRAF3</i> , TNF receptor-associated factor 3	9836800
<i>EEF10</i> , eukaryotic translation elongation factor 10	216099

^a More information on each gene can be found at <http://www.gdb.org/>.

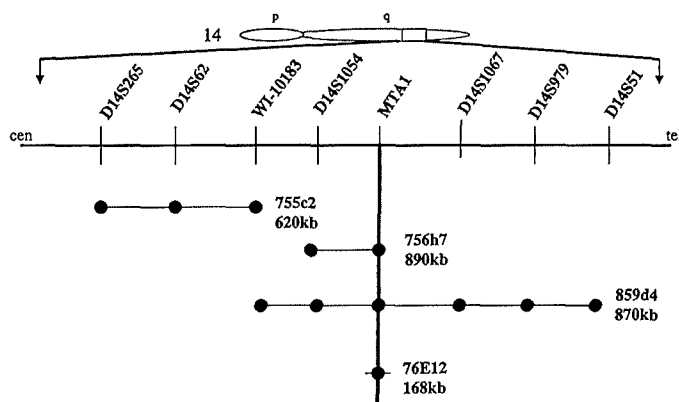


Fig. 1. YAC and BAC mapping of *MTA1*. A 1.6-Mb section of the region of interest was mapped, spanning from marker D14S265 to marker D14S51. The position of *MTA1* is shown relative to other markers on chromosome 14q. *MTA1* was determined to map onto both YAC 756h7 and YAC 859d4 and also to BAC 76E12.

Recently, MTA1 has also been shown to be associated with histone deacetylase activity. Xue *et al.* (11) found that MTA1 was identical to one subunit of the nucleosome remodeling and histone deacetylation complex. This complex contains both ATP-dependent chromatin-remodeling and histone deacetylase activities (12). Interestingly, two homologues of MTA1 have also been discovered. Zhang *et al.* (13, 14) reported that a protein similar to MTA1 was also a component of the nucleosome remodeling and histone deacetylation complex. This gene, since designated *MTA1-L1*, has been cloned and shows significant homology to *MTA1* (15). *MTA1-L1* maps to chromosome 11 on the NCBI Gene Map. An even more distantly related MTA1 homologue, now referred to as *MTA2*, maps to chromosome 2 on the NCBI Gene Map. The MTA1 (and MTA1-L1) proteins are both nuclear proteins containing motifs associated with transcriptional corepressors, gene methylation, and signal transduction (11). All of these observations fit well our model in which LOH of the MTA1 region impedes metastasis. However, because LOH events involve the loss of large segments or entire chromosomes, loss of additional MTA1-region genes (see Table 1) could influence the metastasis phenotype.

References

1. National Cancer Institute. SEER Cancer Statistics Review, 1973-1991. NIH Publ. No. 94-2789. Bethesda, MD: NIH, 1994.
2. O'Connell, P., Hilsenbeck, S., Mohsin, S., Fuqua, S., Clark, G., Osborne, C., and Allred, D. C. Loss of heterozygosity at D14S62 and metastatic potential of breast cancer. *J. Natl. Cancer Inst.*, *91*: 1391-1397, 1999.
3. O'Connell, P., Pekkeli, V., Fuqua, S., Osborne, C. K., and Allred, D. C. Molecular genetic studies of early breast cancer evolution. *Breast Cancer Res. Treat.*, *32*: 5-12, 1994.
4. O'Connell, P., Pekkeli, V., Fuqua, S. A., Osborne, C. K., Clark, G. M., and Allred, D. C. Analysis of loss of heterozygosity in 399 premalignant breast lesions at 15 genetic loci. *J. Natl. Cancer Inst.*, *90*: 697-703, 1998.
5. Toh, Y., Pencil, S. D., and Nicolson, G. L. A novel candidate metastasis-associated gene, *mta1*, differentially expressed in highly metastatic mammary adenocarcinoma cell lines. cDNA cloning, expression, and protein analyses. *J. Biol. Chem.*, *269*: 22958-22963, 1994.
6. Toh, Y., Oki, E., Oda, S., Tokunaga, E., Ohno, S., Maehara, Y., Nicolson, G. L., and Sugimachi, K. Overexpression of the *MTA1* gene in gastrointestinal carcinomas: correlation with invasion and metastasis. *Int. J. Cancer*, *74*: 459-463, 1997.
7. Nawa, A., Nishimori, K., Lin, P., Maki, Y., Mouc, K., Sawada, H., Toh, Y., Fumitaka, K., and Nicolson, G. Tumor metastasis-associated human *MTA1* gene: its deduced protein sequence, localization, and association with breast cancer cell proliferation using antisense phosphorothioate oligonucleotides. *J. Cell. Biochem.*, *79*: 202-212, 2000.
8. Toh, Y., Pencil, S. D., and Nicolson, G. L. Analysis of the complete sequence of the novel metastasis-associated candidate gene, *mta1*, differentially expressed in mammary adenocarcinoma and breast cancer cell lines. *Gene*, *159*: 97-104, 1995.
9. Iguchi, H., Imura, G., Toh, Y., and Ogata, Y. Expression of *MTA1*, a metastasis-associated gene with histone deacetylase activity in pancreatic cancer. *Int. J. Oncol.*, *16*: 1211-1214, 2000.
10. Toh, Y., Kuwano, H., Mori, M., Nicolson, G. L., and Sugimachi, K. Overexpression of metastasis-associated MTA1 mRNA in invasive oesophageal carcinomas. *Br. J. Cancer*, *79*: 1723-1726, 1999.
11. Xue, Y., Wong, J., Moreno, G. T., Young, M. K., Cote, J., and Wang, W. NURD, a novel complex with both ATP-dependent chromatin-remodeling and histone deacetylase activities. *Mol. Cell*, *2*: 851-861, 1998.
12. Toh, Y., Kuninaka, S., Endo, K., Oshiro, T., Ikeda, Y., Nakashima, H., Baba, H., Kohnoe, S., Okamura, T., Nicolson, G. L., and Sugimachi, K. Molecular analysis of a candidate metastasis-associated gene, *MTA1*: possible interaction with histone deacetylase 1. *J. Exp. Clin. Cancer Res.*, *19*: 105-111, 2000.
13. Zhang, Y., LeRoy, G., Seelig, H. P., Lane, W. S., and Reinberg, D. The dermatomyositis-specific autoantigen Mi2 is a component of a complex containing histone deacetylase and nucleosome remodeling activities. *Cell*, *95*: 279-289, 1998.
14. Zhang, Y., Ng, H. H., Erdjument-Bromage, H., Tempst, P., Bird, A., and Reinberg, D. Analysis of the NuRD subunits reveals a histone deacetylase core complex and a connection with DNA methylation. *Genes Dev.*, *13*: 1924-1935, 1999.
15. Futamura, M., Nishimori, H., Shiratsuchi, T., Saji, S., Nakamura, Y., and Tokino, T. Molecular cloning, mapping, and characterization of a novel human gene, *MTA1-L1*, showing homology to a metastasis-associated gene, *MTA1*. *J. Hum. Genet.*, *44*: 52-56, 1999.